Dipartimento di Scienze

Dottorato in Scienze e Tecnologie Biomediche

-XXX ciclo-

"CHOLESTEROL METABOLISM IN AUTISM SPECTRUM DISORDERS"

Ph.D Student: Veronica Cartocci

Tutor: Prof. Valentina Pallottini

Co-Tutor: Dr. Marco Segatto

PhD school coordinator:

Prof. Paolo Visca

INDEX

RIASSUNTO

“METABOLISMO DEL COLESTEROLO NEI DISTURBI DELLO SPETTRO AUTISTICO”

Con il termine “Disturbi dello spettro autistico” si indica un insieme di disturbi del neuro-sviluppo identificabili attraverso specifiche caratteristiche tra cui: la compromissione delle funzioni sociali e comunicative, comportamenti stereotipati, disabilità intellettiva e deficit emotivi.

Solitamente, queste disabilità si manifestano durante l’infanzia, e possono assumere diversi fenotipi, il che rispecchia la natura multi fattoriale tipica dell’autismo. Nonostante sia stata riconosciuta una base genetica nello sviluppo di tale sindrome, sembra sempre più evidente come anche l’esposizione a specifici fattori ambientali, durante la vita prenatale, possa contribuire all’eziologia di questa patologia.

Alcuni studi a riguardo ipotizzano una relazione tra i disturbi dello spettro autistico ed una de-regolazione dell’omeostasi del colesterolo (Wang, 2014). Il colesterolo è un importante lipide, sintetizzato dall’enzima 3β-idrossi 3β-metilglutaril CoA reduttasi (HMGCR) attraverso la via biosintetica del mevalonato (MVA), il quale produce non solo colesterolo ma anche altri importanti prodotti finali come prenili, dolicolo e ubichinone (Buhaescu and Izzedine, 2007). E’ importante sottolineare come la regolazione omeostatica di questa molecola dipenda dal sesso e dall’età, sia nel fegato che nel sistema nervoso centrale (CNS) (De Marinis et al., 2008; Segatto et al., 2013).

Sebbene nel cervello il colesterolo sia regolato dalle stesse proteine che ne regolano l’omeostasi nel resto del corpo, in questo tessuto esso presenta delle peculiarità: i) il colesterolo presente nel CNS è completamente separato dal colesterolo plasmatico, e quindi la sua sintesi avviene *in situ*; ii) nei mammiferi, durante le prime fasi di sviluppo cerebrale, i neuroni hanno la capacità di sintetizzare autonomamente colesterolo, mentre nel periodo post-natale queste cellule riducono o abbandonano la sintesi del lipide, acquisendolo direttamente dagli astrociti (Pfrieger and Ungerer, 2011). Ad oggi, nonostante queste informazioni, rimane ancora poco chiaro se la riduzione di sintesi che si verifica nei neuroni sia una causa o una conseguenza del loro differenziamento. Inoltre, seppure è stata ipotizzata

una correlazione tra i disturbi del neurosviluppo, in particolare dello spettro autistico e il colesterolo, nessuno studio ha mai definito il ruolo della via del MVA e dei suoi prodotti finali in un modello preclinico di autismo. Per queste ragioni, durante il mio periodo di dottorato, ci siamo proposti di raggiungere i seguenti obiettivi:

1) Studiare il ruolo della via del MVA e la modulazione delle proteine regolatrici dell'omeostasi del colesterolo, durante il processo di differenziamento neuronale.
2) Analizzare, in un modello preclinico di autismo, le proteine che regolano l'omeostasi del colesterolo in differenti aree cerebrali a diverse età dello sviluppo.
3) Studiare, nello stesso modello sperimentale se esiste una eventuale differenza di sesso nel metabolismo del colesterolo.

Per raggiungere il primo obiettivo abbiamo studiato i livelli e l'attivazione dell'HMGCR, enzima chiave della via del MVA, in cellule di neuroblastoma N1E-115 durante il loro differenziamento.

I nostri risultati hanno dimostrato che i livelli della reduttasi diminuivano, riducendo di conseguenza la sintesi del lipide, suggerendo che la diminuzione dell'attività della via del MVA possa rappresentare un prerequisito fondamentale per un corretto differenziamento neuronale. A supporto di tale ipotesi, l'inibizione dell'HMGCR mediata da Simvastatina (Sim) induceva un aumento dell'allungamento dei neuriti ed evidenziava un ruolo determinante anche degli altri prodotti finali della via biosintetica, in particolare della proteina geranilata RhoA.

Questi risultati ci hanno suggerito che interferenze nella via metabolica del MVA potrebbero inficiare il corretto differenziamento neuronale ed essere una delle cause alla base dei disordini del neuro-sviluppo, come i disordini dello spettro autistico.

Al fine di approfondire questa ipotesi, abbiamo analizzato le principali proteine coinvolte nella regolazione della via del MVA in un modello sperimentale di autismo, ovvero ratti esposti durante la vita prenatale ad acido valproico (VPA). Gli esperimenti sono stati eseguiti su fegato, plasma e sei aree cerebrali di ratti maschi infanti, adolescenti ed adulti.

I nostri risultati hanno confermato che l'esposizione prenatale al VPA induceva negli animali alterazioni comportamentali riconducibili allo spettro autistico, senza alcuna alterazione nel metabolismo del colesterolo a livello epatico (eccetto un transiente accumulo negli infanti) e plasmatico negli adolescenti e negli adulti. Al contrario, gli studi effettuati su

differenti aree cerebrali, quali ippocampo, corteccia prefrontale, cervelletto, amigdala, striato dorsale e nucleus accumbens riportavano modifiche sia della reduttasi che dei recettori deputati al trasporto del colesterolo. In particolare, ogni area presentava una modulazione indipendente ed età-specifica.

I dati da noi ottenuti evidenziano che l'adolescenza è l'età maggiormente compromessa dal punto di vista dell'attività dell'HMGCR e che vi è una chiara alterazione delle proteine geranilate e farnesilate nel cervelletto e nel nucleus accumbens. Inoltre è riscontrabile una riduzione del contenuto di colesterolo nell'ippocampo dipendente da una riduzione del numero di oligodendrociti.

Infine, poiché, sia l'incidenza dell'autismo che la regolazione dell'omeostasi del colesterolo mostrano differenze legate al sesso, abbiamo verificato se fossero presenti alterazioni del metabolismo del colesterolo dipendenti dal sesso in ratti adolescenti ed adulti, esposti nella vita prenatale al VPA.

I risultati hanno confermato che il VPA non influenza il metabolismo lipidico a livello epatico e plasmatico, mentre nel cervello l'esposizione prenatale a questa sostanza induce un'alterazione sesso ed età specifica.

Nel complesso, i dati ottenuti durante il mio dottorato sottolineano il ruolo chiave della via del MVA nello sviluppo neuronale e suggeriscono che interferenze su questo processo potrebbero indurre alterazioni comportamentali come quelle osservabili nei disordini dello spettro autistico. Inoltre, questi risultati indicano per la prima volta una possibile correlazione tra omeostasi del colesterolo, autismo e differenze dipendenti dal sesso.

SUMMARY

Autism spectrum disorders (ASDs) represent a range of neurodevelopmental pathologies, characterized by impaired social interactions, delay of cognitive functions, compromised communication, repetitive and restricted behaviors, and comorbid features (Faras et al., 2010).

Usually these disabilities affect children during childhood, and present different phenotypes, considering the multi-factorial nature of ASDs. In fact, despite genetic alterations play a role in the development of these disorders, the role of environmental factors, during prenatal life, is becoming an important area of research to find other aspects not yet analyzed, but could be very important to clarify the autism etiology. Interestingly, ASDs have been associated to a loss of cholesterol homeostasis (Tierney, 2008; Wang, 2014). Cholesterol is an important lipid, synthesized by 3β-hydroxy 3β-methylglutharyl Coenzyme A reductase (HMGCR) through the Mevalonate (MVA) pathway that produces, beside cholesterol, other important compounds such as prenyls, dolichol, and ubiquinone. Remarkably, cholesterol homeostasis displays a sex- and age-dependent regulation both in liver and in Central Nervous System (CNS) (De Marinis et al., 2008; Segatto et al., 2013). Moreover, although cholesterol homeostasis in the CNS is regulated by the same protein network operating in peripheral tissues, it presents some peculiarities: i) the cholesterol present into the CNS is completely separated from the rest of the body, thus it is synthesized *in situ*; ii) prenatally in mammals, during brain development, neurons are able to synthesize cholesterol, while postnatal neurons reduce or abandon cholesterol synthesis up-taking it from astrocytes (Martin et al., 2014; Segatto et al., 2014). As far as we know, it is not clear if the reduction of cholesterol synthesis in neurons is a cause or a consequence of neuronal differentiation. Moreover, despite a relation between the neurodevelopmental disorders such as ASDs and cholesterol has been hypothesized, no information are present about MVA pathway and cholesterol homeostasis in a preclinical model of ASDs. For these reasons, the mains goals of my PhD project have been:

1) To study the role of MVA pathway and the modulation of the protein network of cholesterol homeostasis during neuronal differentiation;
2) To study, in an ASDs experimental model, the protein network of cholesterol homeostasis in different brain areas at different age of development;

3) To identify whether sex-related differences are present in the same experimental model of autism.

To start, using differentiated N1E-115 cell line as *in vitro* experimental model, we analyzed the protein network regulating MVA pathway. The results demonstrated that HMGCR levels decreased during neuronal differentiation, suggesting that a physiological downregulation of MVA pathway activation occurs during. HMGCR inhibition by Simvastatin (Sim) supports this notion, as it determined the increase of neurite elongation. Interestingly, this effect was related to a reduced RhoA prenylation/activation.

Overall, these data underlined a key role of MVA pathway in neuronal differentiation, and indicate that the decrease of MVA pathway activity is a cause rather than an effect of this physiological process.

The findings obtained by N1E-115 let us suppose that alterations in MVA pathway could be involved in the onset of neurodevelopmental disorders, such as autism spectrum disorders (ASDs).

In order to delve deeper into this hypothesis, we analyzed the protein network controlling MVA pathway in infant, adolescent and adult male rats prenatally exposed to valproic acid (VPA), a well-established experimental model of autism (Nicolini and Fahnestock, 2017).

We found that prenatal VPA exposure did not alter cholesterol metabolism in both plasma and liver of VPA-animals. On the other hand, disruptions in cholesterol/isoprenoid homeostasis hippocampus, prefrontal cortex, cerebellum, amygdala, dorsal striatum and nucleus accumbens were present in the CNS. In particular, VPA exposure determined a peculiar and distinctive impairment for each brain region. For instance during adolescence, the most affected period by VPA exposure, evident alterations in geranylgeranylated and farnesylated protein levels were observed in the cerebellum, nucleus accumbens and striatum; whereas decreased cholesterol levels were only highlighted in the hippocampus, probably depending on the reduced number of olygodendrocytes found in this brain region.

The incidence of autism, as well as the regulation of cholesterol/isoprenoid metabolism, display typical differences between both sexes. Thus, in the attempt to find additional correlations between autism and perturbations in cholesterol/isoprenoid homeostasis, we verified whether sex-related differences were also present in adolescent and adult male and female rats prenatally exposed to VPA.

Results demonstrated that VPA specifically affected cholesterol/isoprenoid metabolism in the brain, in an age and sex-dependent manner.

Taken together, the results obtained during my PhD studies underlie the pivotal role of MVA pathway in neuronal development, suggesting that any interference in this process could induce behavioral alterations like those ones occurring in ASDs. Moreover, these results suggest for the first time, a possible correlation among cholesterol homeostasis, ASDs and sex.

CHAPTER 1

INTRODUCTION

1.1 AUTISM SPRECTRUM DISORDERS AND BRAIN CHOLESTEROL HOMEOSTASIS

Autism spectrum disorders (ASDs) are a group of diseases characterized by altered sociability, compromised communication skills and stereotyped/repetitive behaviors, appearing usually between 2 and 3 years of age, although there are ASDs cases diagnosed before 24 months of age (Lord et al., 2006; Christensen et al., 2016). Data evidence that 1% of worldwide population is affected by ASDs with higher frequency in USA, where a ratio of 1 case every 68 births is reported. From 2002 to 2010, it has been highlighted a strong increase in ASDs prevalence (from 6 to 15 %). Many studies explain that these disorders are more frequent in male than female with a ratio of 4:1; this result could be related to mechanisms occurring during the sexual development (Vijayakumar and Judy, 2016).

The term "spectrum" reflects the heterogeneous conditions at the base of these pathologies. Specifically, although many studies have tried to connect the mechanisms determining ASDs to genetic, metabolic, epigenetic, hormonal, neuroanatomic, physiologic and environmental alterations, unfortunately only about the 25 % of cases have a clear aetiology (Coleman and Gillberg, 2011; Mintz, 2017). Some research studies also suggest, among the possible causes of ASDs etiology, impairments of cholesterol/isoprenoid metabolism, particularly in the brain. In Smith Lemli Optiz syndrome (SLOS), a developmental disorder belonging to ASDs and caused by the mutation on 7-dehydrocholesterol reductase, improvements of both autistic behaviors and neurodevelopmental status have been evidenced after treatment with dietary cholesterol supplementation (Elias et al., 1997; Tierney, 2008). Moreover, about the 10-15% of people affected by autism present alterations on genes like *FMR1* (*Fragile X Mental Retardation-1*) or *MECP2* (Vijayakumar and Judy, 2016), involved in the Fragile X and Rett syndromes, respectively: both the diseases have been correlated to cholesterol metabolism (Buchovecky et al., 2013; Wang, 2014). Perturbed brain cholesterol metabolism was also found in Asperger Syndrome (AS) where patients can manifest altered lipid levels accompanied by enhanced social anxiety and obsessive-

compulsive symptoms (Dziobek et al., 2007). Similar evidence on cholesterol metabolism alterations have been also found in other non syndromic ASDs, strengthening the hypothesis that disruption of cholesterol homeostasis could play a significant and unexplored role in ASDs condition.

In the Central Nervous System (CNS) cholesterol is localized, with a percentage of 70-85%, in the myelin sheaths surrounding axons, representing one of the main components of neuronal and astrocytes membranes (Morell and Quarles, 1999; Snipes and Orfali, 1998). Oligodendrocytes have a high ability to produce cholesterol respect astrocytes, which synthesize 2-3 times more cholesterol than neurons. It has been postulated that neurons are able to produce cholesterol during the prenatal life, while in the postnatal period they reduce or leave this production by up-taking cholesterol from astrocytes (Mauch et al., 2001; Pfrieger, 2003a). This hypothesis is further supported by recent results from van Deijk and collaborators demonstrating *in vivo* that astrocyte lipid metabolism is critical for proper development of presynaptic terminals and for hippocampal function (van Deijk et al., 2017).

Brain cholesterol is synthesized *in situ*, and represents the 23% of sterols present in the whole body pool although the CNS constitutes 2% of total body weight. Brain cholesterol metabolism is completely separated from the rest of body, since the blood brain barrier (BBB) avoids the passage of cholesterol from the systemic circulation to the CNS and vice versa (Pfrieger, 2003b; Segatto et al., 2012).

When the CNS is completely developed and so the brain cholesterol amount becomes constant, the de novo synthesis of molecole declines and the excess of the lipid is undergone to oxidation process. This process produces the 24-S hydrocholesterol, which cross the BBB at a higher rate than no-oxidized cholesterol (Lutjohann and von Bergmann, 2003).

In the brain, cells require cholesterol for their development and physiologic functions (Segatto et al., 2014a). In particular, neurons need large amounts of this component to form and maintain axons, dendrites and spines and to sustain the function of key membrane proteins like neurotransmitter receptors, ion channels and transporters (Mauch et al., 2001; Pfrieger and Ungerer, 2011). Cholesterol is considered the main component of synaptic vesicles, whose formation, shape, and release properties are controlled by cholesterol content (Segatto et al., 2014b). On the postsynaptic side, cholesterol has a role in the organization and the correct positioning of neurotransmitter receptors. Thus, a reduced

amount of cholesterol on the postsynaptic surface can impair neurotransmission, and induce a loss of dendrite spines and synapses (Sooksawate and Simmonds, 2001).

Moreover, this molecule plays a role in memory and learning processes, since a decreased amount of the lipid can compromise the normal development of brain (Saher et al., 2005).

1.2 CHOLESTEROL BIOSINTHESIS

Cholesterol was discovered in the gallstone in solid form in 1769, found for the first time in blood in 1833 while its structure was determined in 1932 (Olson, 1998). Cholesterol is an amphipathic molecule, characterized by four hydrocarbon rings forming the steroid structure, a hydrophobic tail linked to one end and a hydroxyl group linked to the other end (Enrich et al., 2015; Mitsche et al., 2015). Cholesterol is one of the most important molecule in the cellular physiology both by structural and functional point of view. It is an essential membrane component where regulates the fluidity, thickness, water penetration, and intrinsic curvature of lipid bilayer. Moreover cholesterol is the main precursor of steroid hormones, bile acids, vitamin D (Gillberg et al., 2017).

Cholesterol is transported in the blood within lipoproteins, called apolipoproteins, composed by phospholipids, triglycerides and cholesterol esters. These molecules divided in different classes on the base of their density, are recognized and bound by specific membrane receptors.

The synthesis of cholesterol occurs through the MVA pathway, a metabolic way responsible both of the cholesterol production and isoprenoid molecules as dolichol, ubiquinone (CoQ) and isoprenyl units, all compounds involved in important cellular processes (Buhaescu and Izzedine, 2007) (Figure 1).

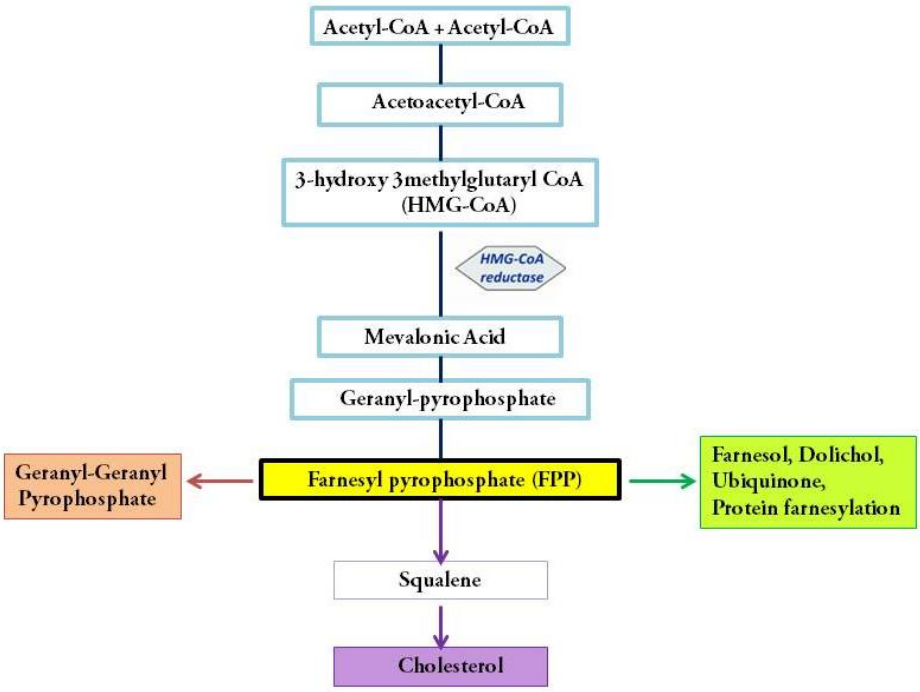

Figure 1. Mevalonate pathway.

The first step of this pathway is characterized by 3-hydroxy 3methylglutharyl Coenzyme A (HMG-CoA) production, after the condensation of three acetyl-CoA units by the acetoacetyl-CoA thiolase and the HMG-CoA synthase action. The subsequent reduction of HMG-CoA to MVA requires the consumption of two NADPH molecules and is mediated by the HMGCR, the main regulatory enzyme in cholesterol biosynthesis, and the most important target of hypocholesterolemic therapies (Lecis and Segatto, 2014).

The first three steps of MVA pathway form the upper MVA pathway (Miziorko, 2011) and are followed by the phosphorylation of MVA, with the transfer of three phosphate groups from three ATP molecules. The phosphate attached to the C-3 hydroxyl group of MVA in the intermediate 3-phospho-5-pyrophosphomevalonate is a good leaving group; in particular the release of both this phosphate and near carboxyl group causes a double bond to produce isopentenyl pyrophosphate (IPP), the first of activated isoprene unit, needed for cholesterol synthesis. IPP is subjected to isomeration process to yield the second activated isoprene unit, the dimethyllalyl pyrophosphate. The farnesil pyrophosphate synthase (FPPS) catalyzes two reactions of IPP and dimethyllalyl condensation to form geranyl pyrophosphate and then 15-carbon intermediate farnesil pyrophosphate (FPP) which represents the main point to provide the biosynthesis of the MVA pathway end-products as cholesterol, dolichol,

ubiquinone and isoprenyl units to regulate the farnesylation and geranylation of proteins (Rozman and Monostory, 2010; Dhar et al., 2013). Two molecules of FPP join head to head, with the elimination of both pyrophosphate groups, to form squalene. The action of squalene monoxygenase determines the production of the squalene 2,3-epoxyde, where the double bounds are positioned so that a reaction transforms the linear molecule in a cyclic structure, the lanosterol, which is converted in cholesterol through 20 reactions.

1.3 OTHER PRODUCTS OF THE MVA PATHWAY

1.3.1 Dolichol

Dolichol is an alpha saturated polyisoprenoid alcohol playing important roles in the synthesis of glycoprotein and in packing and organization of phospholipids (Chojnacki and Dallner, 1988): discovered in 1960, it exists in phosphorylated, dephosphorylated or in esterified form associated with a fatty acid. It is localized mainly in peroxisomes, lysosomes, plasma membrane and Golgi vesicles (Rip et al., 1981) but also in the inner mitochondrial membrane. As phosphorylated dolichol, this compound is an important lipid carrier for the early stage of N-glycosylation process, while, as free alcohol, its role remains still unclear. Moreover, many studies highlight a role both in the regulation of membrane fluidity and structure and in the membrane trafficking, since enhances vesicles fusion (Cantagrel and Lefeber, 2011) (Figure 2).

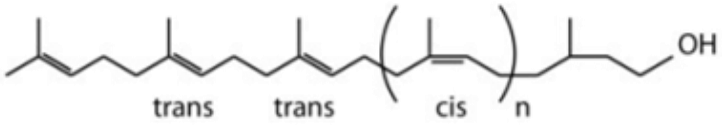

Figure 2. Structure of Dolichol (Rauthan and Pilon, 2011).

1.3.2 Coenzyme Q

Ubiquinone or Coenzyme Q (CoQ) is widely distributed in all cells with an isoprenyl structure different among species. For instance in mammals, including human, it has found mainly as CoQ10 while in rodents prevails the CoQ9 isoform (Nowicka and Kruk, 2010). There are three different redox states of this compound: the full oxidized molecule called ubiquinone, a second form known as semiubiquinone and the full reduced ubiquinol (Brandt, 1999).

CoQ has been characterized in 1955 while its structure has been defined in 1958 (Festenstein et al., 1955). It is the main component of mitochondrial electron transport chain and it is also involved in pathological processes such as inflammation, cardiovascular disease or atherosclerosis (Bentinger et al., 2010; Zhai et al., 2017). CoQ represents the only lipid component of electron transport chain and it is not anchored on the inner mitochondrial membrane, but it moves through the middle of the phospholipid bilayer where the quinone group allows to the ubiquinone to function as an electron-carrier (Turunen et al., 2004) (Figure 3).

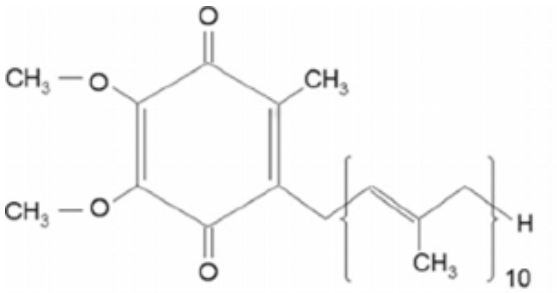

Figure 3. Structure of Coenzyme Q (Figure from Doimo et al., 2014).

1.3.3 Isoprenyl groups

Prenylated proteins are a group of molecules subjected to a post-translational modification, in particular to the binding of either farnesyl (15-carbon) or geranylgeranyl (20-carbon) isoprenoids, on a specific cysteine residue localized near their C-terminus (Shepherd et al., 1995). Three enzymes guide the process: farnesyl transferase, Caax protease and geranylgeranyl transferase I, which are able to recognize a specific short tetra peptide

sequence CAAX on which addict the isoprenyl group (Casey and Seabra, 1996; Wennerberg et al, 2005) (Figure 4).

This lipid modification seems to be indispensable to mediate the membrane interaction of proteins belonging for instance to Ras, Rab and Rho GTPase families but also to determine specific protein-protein interactions and to regulate signal transduction and intracellular trafficking pathways (Zhang et Casey, 1996).

The Ras superfamily, representing the main GTPase family, is divided in five families depending on structural and functional differences: Ras, Rho, Rab, Sar1/Arf and Ran. All members of these families possess a GTPase activity that allows them to hydrolyze GTP. They can exist in two different conformations: an active GTP-bound and an inactive GDP-bound form. Particularly, the activity of these proteins is controlled by the guanine nucleotide exchange factors (GEFs) that remove GDP promoting the GTP-bound form, and GTPase-activating proteins (GAPs) that stimulate the GTP hydrolysis (Bos et al., 2007). The consequence of GTPase/GTP interaction is the association of the prenylated protein to the membrane. This association triggers different signal transduction cascades that regulate cell proliferation or morphology, nuclear or vesicle transport. Moreover, the switch from GDP to GTP of any GTPase proteins results in cytosol or membrane localization (Takai et al., 2001).

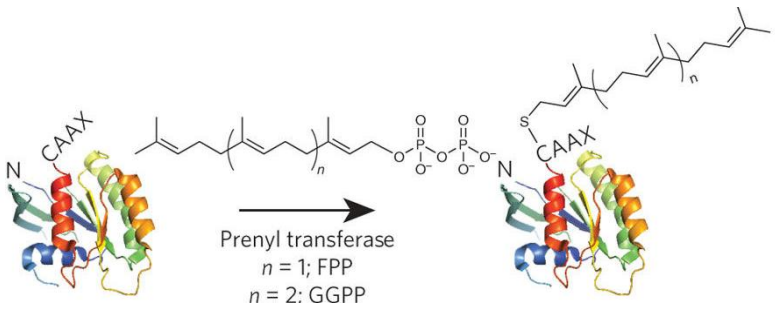

Figure 4. Typical structure of a prenylated proteins, characterized by the addiction of farnesyl or geranylgeranyl residues (isoprenoid chains) to a carboxy-terminal Cys residue of the CAAX sequence (Figure from Hannoush and Sun, 2010).

1.4 PROTEIN INVOLVED IN CHOLESTEROL HOMEOSTASIS

Cholesterol homeostasis is guaranteed through a specific cellular machinery regulated by mechanisms controlling cholesterol biosynthesis, catabolism, transportation, uptake, and depletion which are related to the activity of different proteins and receptors.

1.4.1 3β-hydroxy 3β-methylglutharyl Coenzyme A reductase (HMGCR)

HMGCR is the key enzyme of MVA pathway, catalyzing the conversion of HMG-CoA to MVA, the precursor of cholesterol and other end-products of the metabolic pathway (DeBose-Boyd, 2008).

HMGCR is a transmembrane glycoprotein of 97 kDa anchored to the endoplasmic reticulum (ER). The *HMGCR* gene is located on chromosome 5, map location 5q13.3-5q14, and is over 24.8 kilobases (kb) long. The hydrophobic N-terminal membrane-associated domain (exons 2-10) with 339 residues, anchors the protein to ER membrane and includes a sterol-sensitive domain (SSD) responsible for binding to the sterol and the other end-products of MVA pathway. The hydrophilic cytoplasmic C-terminal domain, the enzyme catalytic region, is linked with N-terminal domain through a linker region of 340-459 residues, representing the third protein domain (Friesen and Rodwell, 2004; Trapani and Pallottini, 2010) (Figure 5).

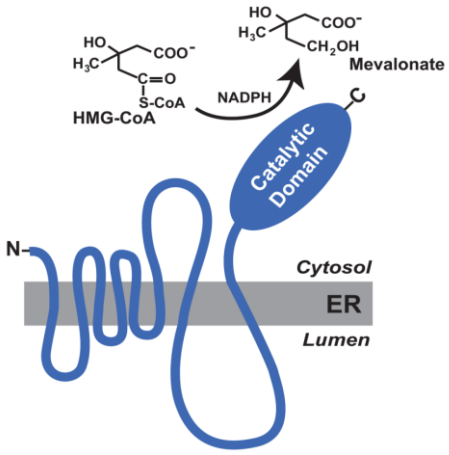

Figure 5. Structural domains of HMGCR. The enzyme is constituted by two domains: the hydrophobic N-terminal domain with eight trans membrane segments, and the hydrophilic C-terminal domain that guides the enzyme activity (Figure from DeBose-Boyd, 2008).

Human HMGCR C-terminal portion forms a tetramer, characterized by individual monomers (Istvan and Deisenholfer, 2000), which are organized into two dimers including two active sites (Istvan and Deisenholfer, 2000) (Figure 6). Each monomer includes three different domains: N-terminal domain connecting the catalytic portion with the membrane domain, L domain or "large" domain, which contains the HMG-CoA binding site, and the S

domain or “small” domain, included in the L domain and forming the NADP(H) binding site (Istvan et al., 2000).

L and S domains, are connected through a beta filament and a “cis-loop”, representing HMG binding site. Coenzyme A links in a positively charged pocket with the portion of pantothenic acid localized inside the protein. NADPH binds a highly conserved pocket constituted by DAMGXN aminoacid sequence (Istvan et al, 2000).

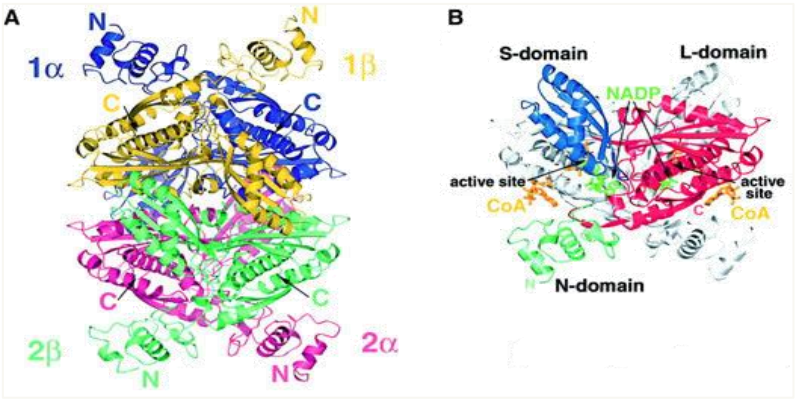

Figure 6. Ribbon diagrams of HMGCR. A) Structure of homotetramer (B) Stereo diagram of the HMGCR dimer structure (Figure from Istvan and Deisenhofer, 2000).

HMGCR short-term regulation is related to phosphorylation/dephosphorylation cycles, determining the inactive or active enzyme state. Although various proteins are involved in this process, the AMP activated Kinase (AMPK) appears to be the major protein involved in this regulatory process. AMPK is a heterotrimeric serin threonin kinase consisting of an alpha catalytic subunit and a beta and a gamma regulative subunits. AMPK activation, occurring with the phosphorylation of threonine 172 within its catalytic subunit (Trapani and Pallottini, 2010), determines HMGCR phosphorylation on serine 872 (S872), and its subsequent inactivation, since phosphorylation induces a low affinity for NADPH.

HMGCR dephosphorylation (responsible for the activation of the enzyme) is operated by Protein Phosphatase 2A (PP2A), a serine/threonine phosphatase, involved in several cellular processes as viral infection cell cycle, cell morphology and development (Segatto et al., 2012) (Figure 7).

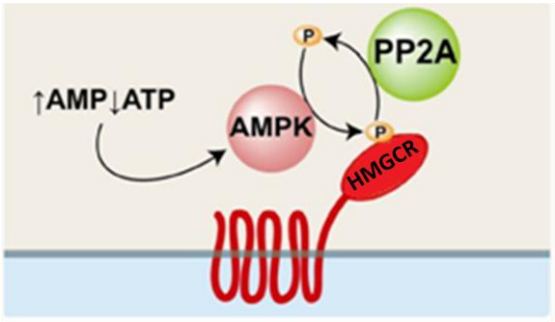

Figure 7. Short-term regulation of mammalian HMGCR catalytic activity by AMP kinase and PP2A (Figure from Burg and Enspenshade, 2011).

The long-term regulation of HMGCR is mediated through transcriptional, translational and post-translational mechanisms: cellular sterols shortage induces the transcription of genes required for cholesterol synthesis and uptake through the action of specific transcriptional factors, called Sterol Regulatory Element Binding Proteins (SREBPs). SREBPs are synthesized as inactive precursor proteins on the ER and their activity is controlled by the sterol-sensing protein Scap (SREBP cleavage-activating protein): in sterol-deprived cells, Scap binds SREBPs mediating the transfer of Scap/SREBPs complex from ER to Golgi where SREBPs are cleaved producing transcriptionally active fragments (nSREBPs). nSREBPs go into the nucleus and transcript their target genes, such as *HMGCR* and *Low Density Lipoprotein receptor* (*LDLr*) (Martini and Pallottini, 2007; Lecis and Segatto, 2014).

In presence of high sterol content, Scap is able to bind another ER resident protein, Insig (Insulin induced gene), this association blocks Scap/SREBP complex inside the ER, preventing SREBPs proteolytic cleavage and gene transcription (Figure 8).

Besides its role in HMGCR transcription, Insig has a role in the degradation of this enzyme throughout two different mechanisms mediated by sterols and the 20-carbon isoprenoid geranylgeraniol (GG). In the first case, sterols stimulate the binding between Insig and HMGCR playing, in this way, a pivotal role in the ubiquitination of the reductase. On the other hand, GG is not involved in the HMGCR ubiquitination but, at the same time, it facilitates its delivery to the proteasome (Sever et al., 2003a; Burg and Espenshade, 2011).

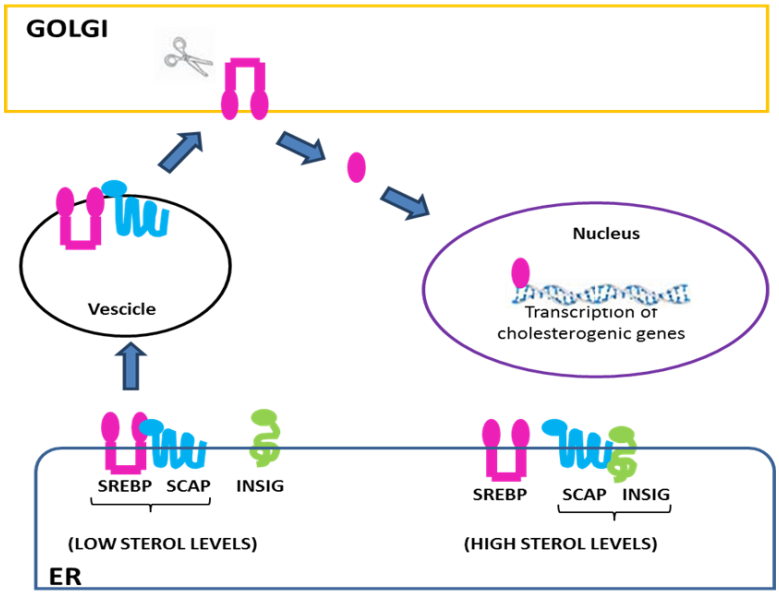

Figure 8. Long term regulation of HMGCR by the cell sterol levels.

1.4.2 Low Density Lipoprotein receptor (LDLr)

Cells are able to acquire cholesterol from the extracellular environment through the activity of different receptors and transporters.

LDLr is a trans-membrane glycoprotein belonging to the Low Density Lipoprotein receptor gene family localized mainly in the liver but also in the other tissues such as adrenal gland and CNS (Harisa and Alanazi, 2014). In humans, the gene is constituted by 18 exons and located to chromosome 19, map location 19p13.2 (Gent and Braakman, 2004). LDLr is the main protein involved in the cholesterol uptake. Specifically, it binds the Low-Density Lipoproteins (LDL) whose degradation allows the cholesterol release from the lipoprotein structure.

The glycosylation of the receptor starts on the membrane of the ER by the insertion of O-linked sugar chains; later, the premature receptor (120 kDa) is transported from ER to Golgi where achieves the mature form by addiction of other O-linked carbohydrate chains (160 kDa). Following this modification, LDLr migrates on the cell surface and binds LDL-particles (Defesche, 2004).

In the mature receptor form are present six different domains: in the N-terminal region, the ligand binding domain is constituted by 292 aminoacids with a cysteine-rich sequence, repeated seven times, that represents the binding site of apoB-100, the apoprotein

synthesized in the liver and contained in LDL (Harisa and Alanazi, 2014; Herz, 2001). Moreover, inside this domain, there are acid chains linking a Ca^{++}; the protonation of these lateral chains determines the release of the metallic ion and the consequent release of LDL from the receptor (Andersen et al., 2003; Herz, 2001). A second region, of 400 aminoacids includes two EGF precursor homology domains (EGFP domains) (Lillis et al., 2008) enriched in serine, threonin and O-linked oligosaccharides and that has a structural role for the binding to LDL (Herz, 2001).

A fourth region has the fifth domain, that presents 22 non-polar residues crossing the membrane, and final region with the sixth domain necessary for the endocytosis of the receptor (Herz, 2001) (Figure 9).

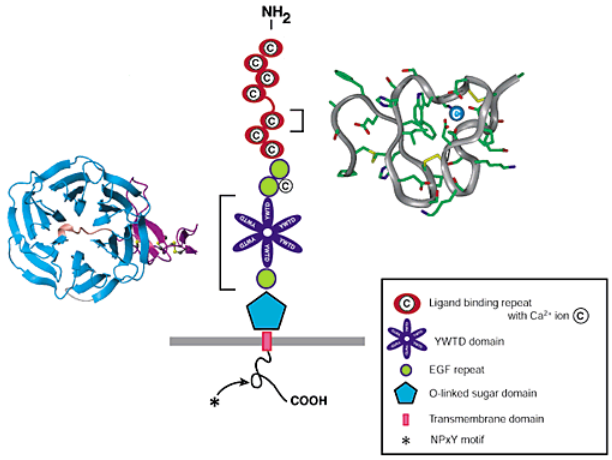

Figure 9. LDL receptor mature structure (Figure modified from Herz, 2001).

1.4.3 Low density lipoprotein receptor Related protein- 1 (LRP-1)

Low density lipoprotein receptor Related Protein-1 (LRP-1) is a component of the LDLr family involved in different cellular processes including lipid and lipoprotein metabolism, activation of lysosomal enzymes, cell growth and migration (Lillis et al, 2005). This receptor uptakes cholesterol binding to apolipoprotein B, the integral component of Very Low Density (VLDL), Intermediate Density (IDL) and Low Density Lipoproteins (LDL) (Lillis et al., 2008).

LRP-1 is present in different cells, especially in neurons. The receptor is synthesized like a big glycosylated trans-membrane protein of 600 kDa that is processed in the trans-Golgi

complex by a convertase. The mature receptor has two subunits non-covalently associated: an extra-cellular α chain, that is the N-terminal fragment of 515 kDa and a cytoplasmic chain, of 85 kDa representing the C-terminal fragment. This receptor is able to bind 85 different ligands, the interaction is mediated by repeated cysteine-rich regions (CR) known as LRP-1 binding region, localized mainly in the α chain (Herz and Strickland, 2001) (Figure 10).

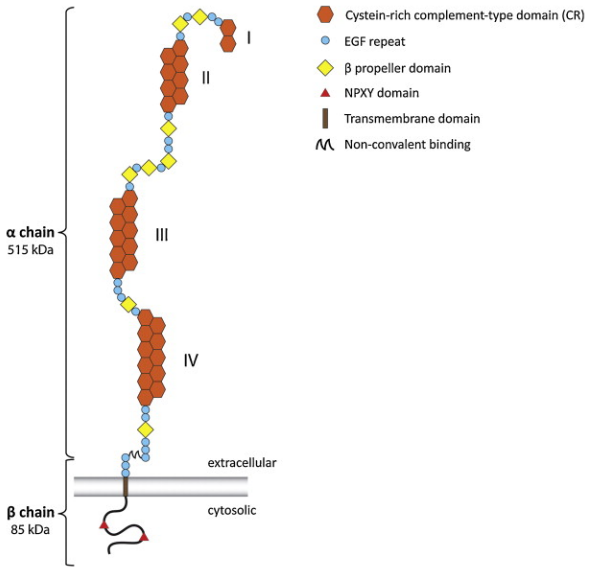

Figure 10. Mature structure of LRP-1 receptor (Figure from Emonard et al, 2014).

Beside the CR regions, the α chain includes EGF homology domains, whose elimination impairs the release of ligands (Emonard et al, 2014).

1.4.4 Scavenger receptor class B type I (SR-B1)

The scavenger receptor class B type 1 (SR-B1) is a plasma membrane receptor, belonging to the group of Scavenger receptors (SRs receptors). Particularly, it is involved in the uptake of High Density lipoprotein Cholesterol (HDL), in the binding of oxidized and Acetylated Low Density Lipoprotein (ox-LDL and Ac-LDL), endogenous proteins and virus and in the bi-directional transport of free cholesterol between HDL and cells (Kinoshita et al., 2004; Valacchi et al, 2011). This molecule is ubiquitously expressed and can be regulated by different processes such as oxidative stress or HCV infection; furthermore, SR-B1 plays a

role in the uptake of lipids and vitamins like vitamin E and is also involved in some pathologies like atherosclerosis, infections, and cancer (Valacchi et al., 2011). SR-B1, whose molecular weight is 82 kDa, contains 509 residues and five domains: a C-terminal domain separated from the N-terminal by a large extracellular domain of 403 amino acid residues, and two trans-membrane domains of 28 and 25 residues that present a site of anchorage in the cytoplasm (Luo et al, 2010). SR-B1 can be glycosylated on 9 different sites and palmitoylated on two cysteine localized on the C-terminal and trans-membrane domain (Krieger, 2001) (Figure 11).

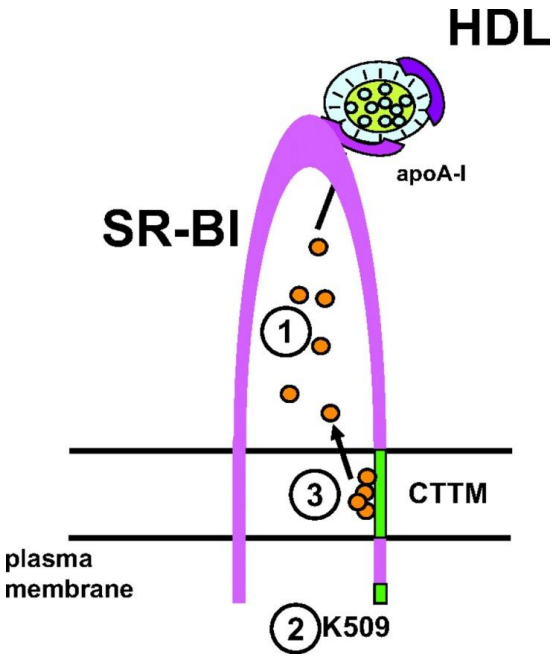

Figure 11. Scavenger receptor B type I (SR-B1): 1 cholesterol flux is responsible of signal initiation, **2** interaction between the C-terminal PDZ-interacting domain and the adapter protein PDZK1 is also needed to induce the activation of the signaling transduction **3** The C-terminal transmembrane domain CTTM is involved in the binding with the plasma membrane cholesterol (Figure from Saddar et al., 2010).

CHAPTER 2

AIM

Autism Spectrum Disorders (ASDs) are neurodevelopmental diseases characterized by impaired social interactions, compromised communication, repetitive behaviors, and comorbid features such as anxiety (Lai et al., 2014; Gillott and Standen, 2007). It has been extensively demonstrated that ASDs may be caused by a set of endogenous factors as, for example, genetic alterations, or exogenous/environmental factors such as the exposure to environmental pollution and drugs, during prenatal and postnatal period. Moreover, it is known that these disorders are more frequently diagnosed in male than female with a ratio of 4:1, evidencing a sex-dependent onset of the disease (Werling and Geschwind, 2013; Vijayakumar and Judy, 2016). Interestingly, also MVA pathway displays a sex-dependent regulation both in hepatic tissue and in CNS (De Marinis 2008; Segatto et al 2012).

It has been hypothesized a possible relationship between neurodevelopmental diseases, such as ASDs, and alterations in brain cholesterol homeostasis, whose function in the maintenance of several neuronal processes is extremely important (Gillberg et al., 2017; Pfrieger, 2003b) but, despite epidemiological data evidence a possible correlation between autism and alterations of cholesterol metabolism, no systematic studies analyzing this relationship at preclinical level have been ever performed.

Thus, our first aim was to investigate the possible involvement of MVA pathway in neuron development. To accomplish this aim, we used an *in vitro* experimental model, the N1E-115 cells, a mouse neuroblastoma induced to differentiate.

Our second aim was to study the possible modulation of cholesterol metabolism, in a well-established animal model of autism: rats prenatally exposed to valproic acid (VPA). The experiments were performed on male rats at three different developmental stages (infancy, adolescence and adult age). At last, our third aim was to study the putative sex-dependent alterations of brain cholesterol metabolism using male and female adolescent and adult rats prenatally exposed to VPA.

CHAPTER 3

MATERIALS AND METHODS

Chemicals and antibodies

Unless indicated otherwise, all materials were from Sigma–Aldrich (St. Louis, MO, USA). Geranylgeraniol (GG) was a generous gift of Prof. Ewa Sviezewszka (Polish Academy of Science, Warsaw, Poland). For immunoblotting, antibodies against the following proteins were used: P-AMPKα and AMPKα (Cell Signalling Technology, Boston, MA, USA), PP2A (catalytic sub-unit), RhoA, Ras, MBP, LRP-1, and SREBP-1 (Santa Cruz Biotechnology, Santa Cruz, CA, USA), LDLr and SREBP-2 (Abcam, Cambridge, UK), P-HMGCR (Millipore, Temecula, CA), HMGCR (Upstate, Lake Placid, NY), SR-B1 (Novus Biological, Littleton, CO, USA). α-Tubulin and vinculin (Sigma–Aldrich) or caveolin (Santa Cruz, CA, USA) were used as loading controls. HRP-conjugated IgG produced in mouse or in rabbit used as secondary antibodies were obtained from Biorad Laboratories (Milan, Italy).

Cell cultures

Mouse neuroblastoma clone N1E-115 was obtained from the European Collection of Cell Cultures (Cat. N°. 88112303) (Salisbury, UK). Cells were grown in Dulbecco's modified Eagle's medium (DMEM) containing 4500 mg/L glucose, 2 mM L-glutamine, 10% fetal bovine serum (FBS), penicillin and streptomycin (Lonza, Milano, Italia) in a humidified incubator with 5% CO2 at 37°C.

Neuronal Differentiation

N1E-115 cells were plated for 5 h in DMEM medium (GIBCO) 10% serum to allow cell adhesion. Neuronal differentiation was induced by the addition of 2% dimethylsulfoxide (DMSO). The medium containing DMSO was changed on day 3 and neuronal

differentiation was observed up to 120 h in the differentiation medium. For experimental treatments, cultures were incubated in the presence of differentiation medium supplemented with Ethanol (Et-OH) as control or with Simvastatin (Sim). In addition culture dishes were treated with different products of the MVA pathway: Cholesterol (CHOL), Farnesol (Far), Geranylgeraniol (GG) in the presence or absence of Sim. These pharmacological agents were used at a concentration of 1 µM dissolved in Et-OH.

Neurite extension assay

The degree of differentiation was evaluated based on the length of neuritic processes in different directions and at different time intervals (16 h, 24 h, 48 h, 72 h 120 h) using an Olympus CKX 41 microscope equipped with a Leica DFC 420 camera. Electronic images were further processed using Adobe Photoshop CS2.

For each treatment, 10 randomly selected fields from 3 independent preparations were analyzed.

While small and spherical in their undifferentiated state, morphologically transformed N1E-115 cells are typically 40 µm or larger and extend processes which often span several hundred µm. The neurite length was evaluated with ImageJ software for Windows (NIH, Bethesda, MD, USA) and was reported as arbitrary units. Only neuritic processes that were longer than two times the diameter of the cell were considered.

XTT assay

Cell viability was detected by the XTT assay following manufacturer instructions (Cell Signalling Technology; Boston, MA, USA). This assay detects a formazan dye produced from XTT conversion by mitochondrial enzymes. 5 X 10^3 cells were plated in 96 well dishes. Cells were treated with 2% DMSO in presence and in absence of 1 µM Sim for 120 h using Et-OH as control.

Flow Cytometry Analysis

To evaluate cell viability, $1.5X10^5$ N1E-115 cells were grown in 3.5 cm Petri dish in DMEM medium (GIBCO) with 10 % FBS and treated with 2% DMSO in the presence of 1 µM Sim or of Et-OH alone (0.1% v/v) for 120 h. After trypsin detach, cells were treated with Propidium Iodide (PI) (2 µg/ml) and immediately analyzed by flow cytometry. For each experiment, 20.000 events on were acquired and the percentage of live cells was calculated by design an electronic gate on PI negative events. To stain SR-B1 on the live cell surface, 1.5 x 10^5 cells were seeded into 3,5 cm Petri dish on DMEM supplemented with 10% FBS for each experimental point. After 5 h, medium was replaced by fresh complete medium containing 2 % DMSO or Et-OH. For each time point (t_0, t_{72}), cells were harvested with trypsin and washed twice with cold phosphate buffered saline (PBS) containing 5 % BSA. For each sample, living cells were incubated with anti-SR-B1 (for 30 min at 4°C; 1:100 in PBS/5% BSA; Novus Biological). Samples were incubated with FITC-conjugated goat anti-rabbit secondary antibody (30 min at 4°C; 1:100 PBS/5% BSA; Cappel). Background controls with secondary antibody alone were included at each time point. Immunofluorescence intensity was measured by a Galaxy flow cytometer (DakoCytomation) and analyzed by Flowjo v.5.4.4 software (Tree Star Inc., Ashland, OR). For each sample, 20,000 events were recorded, data were obtained from three independent experiments. Dead cells were omitted from analysis by side scatter electronic gate exclusion.

Western blotting analysis

To prepare total protein lysate, N1E-115 cells were washed at indicated times with 1 ml of phosphate buffered saline (PBS; PH=7.4), trypsinized (2 min at 37°C), harvested, centrifuged (1 min at 13,000 rpm at room temperature), resuspended and sonicated (30 sec) in 50 µl of sample buffer containing 0.125 M TrisHCl pH 6.8, 10% SDS, 0.062 M NaF and Protease Inhibitor Cocktail (Sigma).

To prepare the membrane fraction, cells were homogenized in a homogenization buffer (0.01 M Tris-HCl, 0.001 M $CaCl_2$, 0.15 M NaCl, 0.001 M PMSF, pH 7.5) and spun down (10,000 g for 10 min). The supernatant was centrifuged two times (100,000 g for 45 min), the pellet containing the membrane fraction was solubilized (0.125 M Tris-HCl -pH 6.8-containing 10% SDS, 0.001 M PMSF) and the protein concentration was measured (Lowry

et al., 1951). Total lysate of livers or different brain regions (Amy, Cereb, Cortex, Hippo, Nac and Str) were obtained by tissue homogenization in respectively 1:10 and 1:5 w/v buffer containing 0.001 M Tris-HCl, 0.0001 M $CaCl_2$, 0.15 M NaCl, and 0.001 M phenylmethylsulfonyl fluoride (PMSF) (pH 7.5), and Phosphatase inhibitor 1:1000 v/v (SigmaAldrich, Milano). Livers and brain samples were sonicated (VCX 130 PB, Sonics, Newtown, 06470 CT) on ice, for 1 min. Successively, for both the tissues, an aliquot of homogenate was diluted 1:1 in sample buffer 2X (0.25 M Tris-HCl pH 6.8, 20% SDS and 1:1000 protease inhibitor cocktail and 1:1000 phosphatase inhibitor cocktail (Sigma-Aldrich) (Pallottini et al., 2008).

Membrane and total lysate samples were boiled for 3 min before SDS-PAGE and subsequent Western blotting. The presence of caveolin (membrane marker) and α-tubulin (cytosolic marker) confirmed the purity of the cellular fractions (data not shown). All experiments were carried out in triplicate. Thirty micrograms of protein were separated by SDS-PAGE and blotted to nitrocellulose membranes (Trans-blott Turbo, BioRad). Immunoblots were incubated with primary antibodies (1:1,000) followed by secondary peroxidase-conjugated antibodies (1:10,000; Biorad). Immunoreactivity was detected by enhanced chemiluminescence (GE Healthcare, Little Chalfont, UK). All images derived from Western blotting were analyzed with ImageJ (National Institutes of Health, Bethesda, MD). Intensity values of selected proteins were normalized to intensities of respective housekeeping proteins (tubulin, vinculin or caveolin).

HMGCR activity assay

Activity was measured using a radioisotopic assay based on the production of ^{14}C-MVA (mevalonate) from 3-[^{14}C]-HMGCoA (specific activity 57.0 mCi/mmol. Amersham-Pharmacia, Little Chalfont, UK). N1E-115 cells were differentiated with 2% DMSO for 120 h in the presence of 1 μM Sim or of Et-OH. Cells were homogenized in phosphate buffer (0.1 M sucrose, 0.05 M KCl, 0.04 M KH2PO4, 0.03 M EDTA, 50 mM NaF, pH 7.4) and incubated in the presence of co-factors (20 mM glucose-6-phosphate, 20 mM NADP sodium salt, 1 unit of glucose-6-phosphate dehydrogenase, and 5 mM dithiothreitol) in a final volume of 190 ml (for 100 μg protein). The assay was started by addition of 10 μl 3-[^{14}C]-HMG-CoA (0.088 mCi/11.7 nmol). The synthesized [^{14}C]-MVA was purified by

chromatography (AG1-X8 ion exchange resin; BioRad, Italy) and the radioactivity measured (Liquid Scintillator Analyzer, Perkin Elmer). The recovery was calculated based on an internal standard (3-[^{3}H]-MVA, specific activity 24.0 Ci/mmol (Amersham-Pharmacia, Little Chalfont, UK).

Filipin staining

5X 10^{3} cells were seeded into 96 wells plate (Falcon black/clear tissue culture treated plate flat bottom) and after adhesion (5 h) the medium was changed with complete medium in presence of 2% DMSO with or without 1 µM of Sim. The medium was changed with fresh stimuli each 2 days and cells were cultured for 120 h. To visualize the intracellular cholesterol distribution, cultured cells were fixed (4% paraformaldehyde for 15 min) and incubated for 2 h with filipin (10 µg/ml with 0.1% Et-OH, Sigma). Filipin fluorescence was imaged on an inverted microscope (Axiovert 135TV; Zeiss) equipped with a metal halide lamp (10%; Lumen 200; Prior Scientific), an appropriate excitation/emission filter (XF02-2; Omega Optical Inc.), a 40x objective (N.A. 1.3; Zeiss) and an air-cooled monochrome CCD camera (Sensicam, PCO Computer Optics) controlled by custom-written Labview routines (National Instruments).
Data analysis was performed with ImageJ (National Institutes of Health, Bethesda, MD) software for Windows. The experiment was performed with four biological replicates. For each experimental group 10 randomly selected fields were analyzed.

Animals

Female Wistar rats (Charles River), weighing 250 ± 15 g, were mated overnight. The morning when spermatozoa were found was designated as gestational day 1 (GD1). Pregnant rats were singly housed in Macrolon cages (40 l x 26 w x 20 h cm), under controlled conditions (temperature 20–21°C, 55–65% relative humidity and 12/12 h light cycle with lights on at 07:00 a.m.). Food (standard laboratory diet, VRF1 (P) diet, Special Diets Services, Charles River) and water were available *ad libitum*. On gestational day 12.5, females received a single intraperitoneal injection of either sodium valproate (VPA) or saline (SAL). Newborn litters found up to 5 p.m. were considered to be born on that day designated postnatal day (PND) 0. On PND 1, the litters were culled to eight animals (six

males and two females), in order to reduce the litter size-induced variability in the growth and development of pups during the postnatal period. On PND 21, the pups were weaned and housed in groups of three. Experiments were carried out on the male offspring during infancy (PNDs 9-13), adolescence (PND 35), and adulthood (PND 90). The experiments were approved by the Italian Ministry of Health (Rome, Italy) and performed in agreement with the guidelines released by the Italian Ministry of Health (D.L. 26/14) and the European Community Directive 2010/63/EU.

Drugs

VPA (Cayman) was dissolved in saline at a concentration of 250 mg/ml and administered intraperitoneally to pregnant rats at a dose (500 mg/kg) and time (GD 12.5) that have been shown to induce autistic-like behavioral changes in the offspring (Markram et al., 2008; Servadio et al., 2016).

Isolation-induced ultrasonic vocalizations (USVs)

On PND 9, 12 male pups (6 SAL- and 6 VPA-exposed) were removed from the nest and individually placed into a Plexiglas arena (30 l × 30 w × 30h cm), located inside a sound-attenuating and temperature-controlled chamber, with a camera positioned above the arena. The USVs emitted by the pup were detected for 3 min by an ultrasound microphone (Avisoft Bioacoustics, Version 5.1) sensitive to frequencies between 10 and 200 kHz. Pup axillary temperature was measured before and after the test by a digital thermometer.

Three-chamber test

The apparatus consisted of a rectangular three-chamber box with two lateral chambers (30 l × 35 w × 35 h cm) connected to a central chamber (15 l × 35 w × 35h cm). Each lateral chamber contained a small Plexiglas cylindrical cage. The test was performed as previously described (Moy et al., 2007; Servadio et al., 2016). At PND 35 or 90, 12 male rats (6 SAL- and 6 VPA-exposed) were individually allowed to explore the apparatus for 10 min, and

then confined to the central compartment. An unfamiliar stimulus animal was placed into the Plexiglas cage in one chamber of the apparatus, while the cage in the other chamber was left empty. Both doors to the side chambers were then opened, allowing the experimental animal to freely explore the apparatus for 10 min. The percent of time spent in social approach (sniffing the stimulus and the cage confining it) was scored using the Observer 3.0 software (Noldus Information Technology, The Netherlands).

Elevated plus-maze

The apparatus comprised two open and two closed arms (50 l × 10 w × 40 h cm) that extended from a common central platform (10 l × 10 w cm). At PND 35, 12 male rats (6 SAL- and 6 VPA-exposed) were individually placed on the central platform of the maze for 5 min. Each session was recorded with a camera positioned above the apparatus for subsequent behavioral analysis performed using the Observer 3.0 software (Noldus Information Technology, The Netherlands). The following parameters were analyzed (Manduca et al., 2015): 1) the percentage of time spent in the open arms (% TO): (seconds spent on the open arms of the maze/seconds spent on the open + closed arms) x 100; 2) the percentage of open arm entries (% OE): (the number of entries into the open arms of the maze/number of entries into open + closed arms) x 100 and 3) the number of closed arm entries (Number of CE).

Samples collection

Infant (n=12, 6 SAL and 6 VPA), adolescent (n=12, 6 SAL and 6 VPA), and adult (n=12, 6 SAL and 6 VPA) rats were rapidly decapitated. Plasma was obtained from blood collected into EDTA (Ethylenediaminetetraacetic acid; 1 mg/ml blood), and livers and brains were quickly removed. For biochemical evaluations, brains were cut into coronal slices on a cold plate, and amygdala (Amy), cerebellum (Cereb) prefrontal cortex (Cortex), hippocampus (Hippo), nucleus accumbens (Nac), and dorsal striatum (Str) were dissected under the stereo-microscope within 2 min. Tissues were then stored to -80°C until use (Trezza et al., 2012). For immunohistochemical analysis whole brains were rapidly frozen in 2-methylbutane and stored at -80°C.

Immunohistochemistry

The staining was performed as described (Scuderi et al., 2014). Briefly, rats were perfused intracardially and brains were cut using a cryostat to obtain coronal sections containing the hippocampal regions. Slices (12 µm thickness) were post-fixed for 7 min in 4% paraformaldehyde prepared in 0.1 M phosphate buffer solution (PBS) at +4°C. Non-specific antibody binding was minimized by incubating slices (placed in a humid chamber) with a blocking solution composed of bovine serum albumin (BSA) 0.5% in PBS/triton X-100 0,25% for 1 h at room temperature. Then, slices were incubated overnight at +4°C in a humid chamber, with a mouse anti-Olig2 primary antibody sc 293163 (1:500) (Santa Cruz Biotechnology) prepared in the same blocking solution. The day after, sections were incubated with the proper rhodamine (TRITC)-coupled goat anti-mouse IgG (H+L) secondary antibody 115-025-003 (1:200) (Jackson ImmunoResearch) and with the nuclear stain Hoechst 33258 (1:5000) (Sigma-Aldrich) in blocking solution at room temperature. Then, sections were rinsed in PBS and slices mounted in Fluoromount medium F4680 (Sigma-Aldrich). Signals were detected using an epifluorescent microscope Eclipse E600 (Nikon). Pictures were captured in the stratum radiatum of CA1, CA2 and CA3, and in the hilus of the dentate gyrus (DG) in the hippocampus by a QImaging camera with NIS-Elements BR 3.2 64-bit software. Experiments were performed three times; at least four slices from each animal were analysed. In particular, we used slices corresponding to plates 55–64 in the rat brain atlas (Paxinos and Watson, 2007).

Tissue and plasma lipid analysis

Total cholesterol and high-density lipoproteins (HDL) were evaluated in plasma samples. Lipid analyses were performed by a Roche Clinical Chemistry instrument with commercial reagents (Roche Diagnostics, GmbH). To evaluate the amount of tissue cholesterol, 50 mg and 25 mg of liver and brain areas, respectively, were homogenized in chloroform:methanol:H_2O 4:2:1 v/v. The mixture was vortexed for 2 min, left for 15 min at room temperature and spun-down (10 min at 600 g). The chloroform fraction was transferred, dried under nitrogen, dissolved in 40 µl isopropanol and subjected separated by thin layer chromatography (Silica Gel 60 Å 5X20, Whatman, Maidston, England; pre-activated at 100°C for 60 min). Samples were developed in petroleum ether/ethyl

ether/acetic acid (75:25:1 v/v) and lipid bands were visualized with iodine vapor and compared with cholesterol standard.

Statistical analysis

Data are expressed as mean ± SD for all the data except for behavioral analyses and immunohistochemistry experiments. In the case of two experimental conditions 6 SAL- and 6 VPA-treated samples for one age and one brain area (or liver tissue) on the same gel/Western blot have been analyzed. These experiments were performed in duplicate from which I calculated mean values, then the Student's t test have been performed comparing SAL and VPA. $p<0.05$ was considered significant (GraphPad Instat3; GraphPad, Inc., La Jolla, CA). Regarding, the experiments with multiple conditions, I evaluated data by one-way analysis of variance (ANOVA) followed by Tukey-Kramer post-test.

CHAPTER 4

RESULTS

4.1 Modulation of the isoprenoid/cholesterol biosynthetic pathway during neuronal differentiation in vitro

(Cartocci et al., 2016 Journal of Cellular Biochemistry)

Our first aim was to investigate the physiological role of the MVA pathway in neuron development. To accomplish it, we used the mouse neuroblastoma cell line N1E-115 as experimental model.

Although the classical differentiation protocol is based on serum deprivation, to avoid cholesterol alterations, we induced neuronal differentiation by using only DMSO (Clejan et al., 1996; Rodrigues et al., 2005; Oh et al., 2006). As a first step, we investigated whether DMSO affected HMGCR. As shown in Figure 12a the protein amount of total HMGCR in N1E-115 decreased, whereas the phosphorylated fraction increased during differentiation. The levels of enzymes that regulate the phosphorylation status of HMGCR, AMPK and PP2A, were stable during 120 h of treatment (Figure 12b). The observed changes in HMGCR suggested that the level of the enzyme decreases during DMSO-induced differentiation. Indeed, metabolic labeling of MVA revealed that its activity was significantly reduced after induction of differentiation (Figure 12 inset), indicating that the metabolic flux through the MVA pathway decreases.

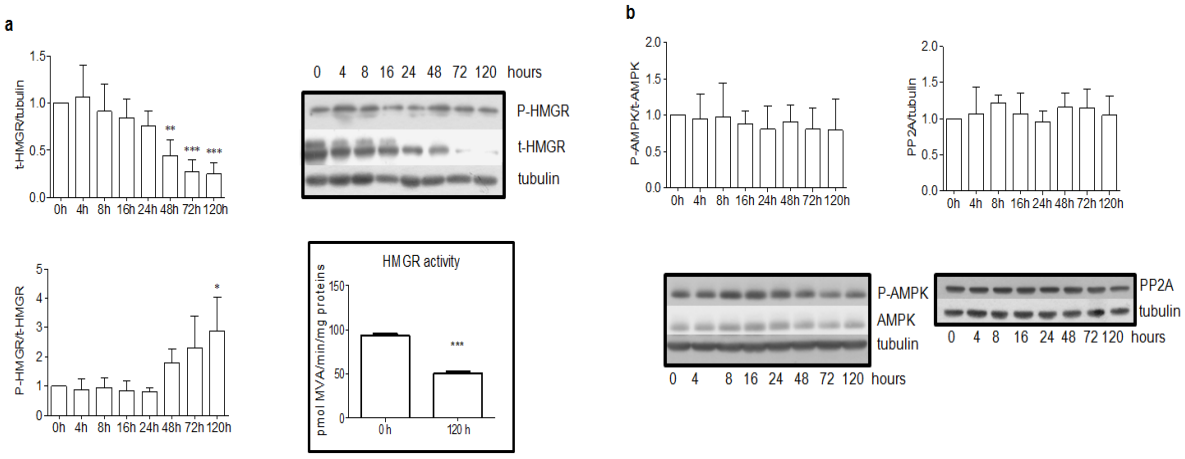

Figure 12. HMGCR, AMPK, and PP2A analysis in differentiating N1E-115 mouse neuroblastoma. Panel **a** illustrates HMGCR analysis. On the left the densitometric analysis of total protein content (up) and the phosphorylation state of the enzyme (bottom), quantified as t-HMGCR/tubulin and P-HMGCR/t-HMGCR, respectively. A representative Western blot is shown on the right (up). **=P<0.01, ***=P<0.001 vs. 0 h as from one-way analysis of variance (ANOVA) followed by Tukey post-test. Inset illustrates HMGCR activity measured as pmol of [^{14}C]-MVA production/min/mg proteins at 0 h and 120 h after the induction of differentiation by using 2% DMSO. ***=P<0.001 vs. 0 h as from a Student's t test. Panel **b** illustrates AMPK (left) and PP2A catalytic sub-unit (right) analysis. On the bottom are represented the immunoblots from representative experiments. Average protein expression is quantified as P-AMPK/AMPK, and PP2A/tubulin (right graph). All the presented data derives from 3 independent experiments, for details see the main text.

The MVA pathway is an important process regulating lipid homeostasis in cells, together with the machinery that mediates cholesterol uptake. We therefore tested whether lipoprotein receptors were affected by DMSO-induced neuronal differentiation. The level of LDLr decreased, whereas the level of LRP-1 was increased (Figure 13a-b). The latter change was not surprising, because LRP-1 is a prominent component of neurites (Kanekiyo and Bu, 2014), whose growth is induced by DMSO.

On the other hand, we also observed a decrease of SR-B1 at 75 kDa (Figure 13c), and interestingly, we observed at 72 h of treatment a band at 150 kDa which may signify the dimerization of SR-B1 and a possible translocation of the protein complex on plasma membrane. The appearance of SR-B1 on the cell surface after 72 h of treatment was confirmed by live labeling with the antibody and subsequent flow cytometric analyses (Figure 13d).

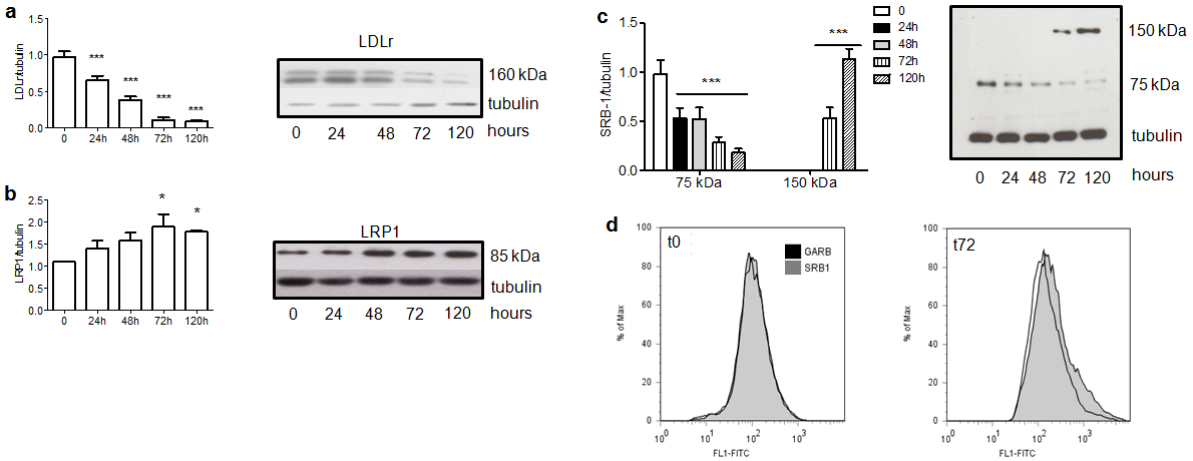

Figure 13. LDLr, LRP-1, and SR-B1 analysis in differentiating N1E-115 mouse neuroblastoma. Panel **a** illustrates LDLr analysis, Panel **b** illustrates LRP-1 analysis, and Panel **c** illustrates SR-B1 analysis. On the right are represented the immunoblots from representative experiments. Average protein expression is represented on the left and quantified as ratio between protein and tubulin. *=P<0.05, ***=P<0.001 vs. 0 h as from one-way analysis of variance (ANOVA) followed by Tukey post-test.
Panel **d** shows membrane expression of SR-B1 receptor on live cells before and after 72 h of DMSO-induced differentiation. The results are presented as cytometric histograms distribution (goat anti-rabbit FITC conjugated control stain (black), versus surface anti-SR-B1 antibody (gray)). These results are representative of three similar experiments.

The expression of MVA enzymes, lipoprotein receptors and other components controlling lipid homeostasis is regulated by the transcription factors SREBP-1 and -2, which undergo cleavage and transfer to the nucleus upon declining lipid levels.

Immunoblot revealed that the levels of transcriptionally active SREBP-1 and of SREBP-2 decreased during differentiation (Figure 14).

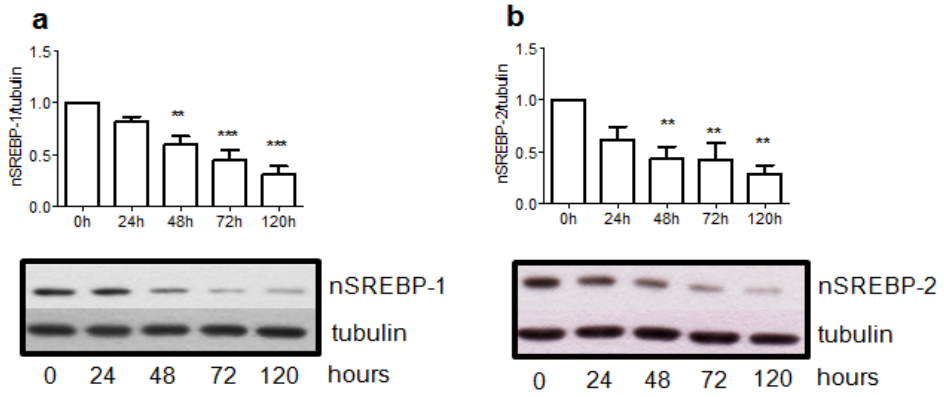

Figure 14. SREBP-1 and SREBP-2 analysis, in differentiating N1E-115 mouse neuroblastoma. Panel **a** illustrates the transcriptionally active fragment of SREBP-1 (nSREBP-1) analysis, Panel **b** illustrates transcriptionally active fragment of SREBP-2 (nSREBP-2) analysis. On the bottom are represented the immunoblots from a representative experiment. Similar results were obtained from three independent experiments for each protein considered. Average protein expression quantified as ratio between protein and tubulin. **=P<0.01, ***=P<0.001 vs. 0 h as from one-way analysis of variance (ANOVA) followed by Tukey post-test.

Our results indicated that neuronal differentiation is accompanied by a decrease in MVA synthesis and predicted that a further decrease of MVA synthesis could accelerate neuronal differentiation. To test this hypothesis, we induced neuronal differentiation by DMSO in presence or absence of Sim, a well-established HMGCR inhibitor, at a concentration that was not toxic to neurons as indicated by XTT and PI exclusion test (Figure 15).

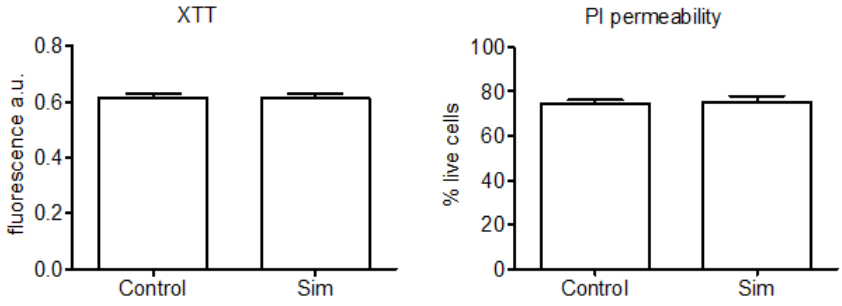

Figure 15. Evaluation of cell viability in differentiating N1E-115 mouse neuroblastoma cells. Figure illustrates on the left XTT assay and on the right PI exclusion assay performed on N1E-115 cells induced to differentiate with 2% DMSO for 120 h in presence and in absence of 1 µM Sim. For details see the main text.

To determine the degree of neuronal differentiation, we measured neurite length. We observed that Sim treatment increased the length of neurites indicating that a decrease of MVA pathway promotes neuronal differentiation in our experimental model (Figure 16a-b).
We next tested which end-product of MVA pathway mediated this effect. We induced neuronal differentiation by means of Sim and added MVA, CHOL, GG or Far for 120 h. As shown in Figure 16c, only MVA and GG prevented Sim-induced increase of neurite outgrowth, suggesting that other end-products, such as Far or CHOL did not mediate this morphological change.

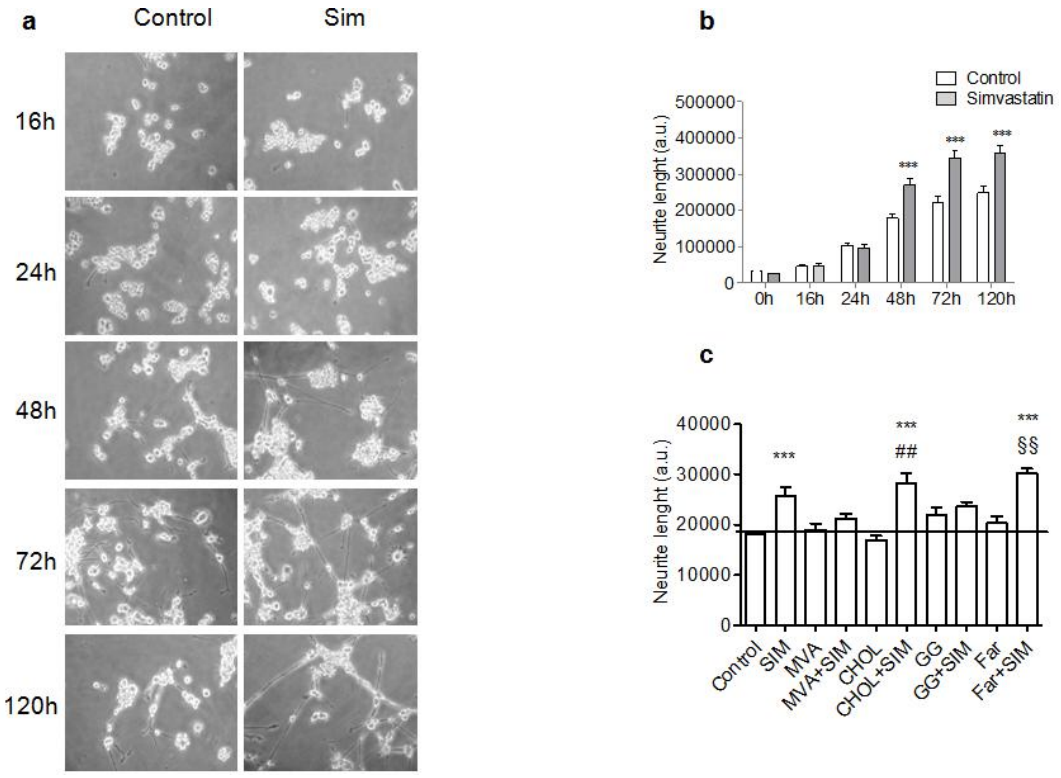

Figure 16. Neurite elongation analysis of N1E-115 mouse neuroblastoma during DMSO-induced differentiation. Panel **a** shows representative pictures of "in vivo" cell detection under an Olympus CKX 41 microscope, equipped with a Leica DFC 420 camera. It represents the neurite elongation during DMSO-induced cell differentiation in presence and in absence of 1 µM Sim starting from 0 h to 120 h. Panel **b** shows the statistical analysis of neurite elongation performed on 10 randomly selected fields from 3 independent preparations. Panel **c** represents the neurite elongation analysis, at 120 h after the induction of the differentiation by DMSO, in presence and in absence of Sim or Sim + HMGCR end products: MVA, CHOL, GG, Far. All the compounds were administered at 1 µM. The analysis was performed on 10 randomly selected fields from 3 independent preparations. ***=P<0.001 vs. Control, ##=P<0.01 vs. CHOL, §§=P<0.01 vs Far; as from one-way analysis of variance (ANOVA) followed by Tukey post-test.

Supporting this notion, filipin staining demonstrated that cellular cholesterol content is not affected, as no differences were detectable between vehicle- and Sim-treated cells (Figure 17).

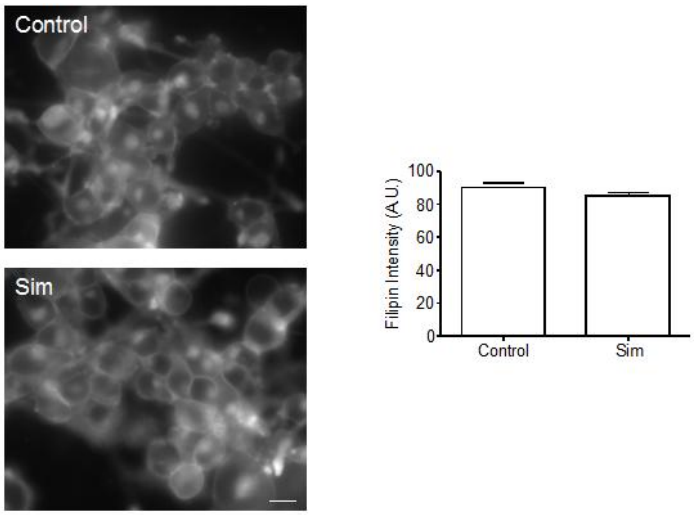

Figure 17. Cholesterol content evaluation in differentiating N1E-115 mouse neuroblastoma. N1E-115 cells were treated or not with 1 μM Sim, for 120 h after DMSO administration. Cells were fixed with 4% paraformaldehyde and stained with filipin. Representative pictures of the filipin staining are shown on the top. On bottom, data analysis of filipin intensity measured as described in the main text is illustrated.

GG is required for the prenylation of GTP binding proteins and prominent targets are the Rho family GTPases. A prominent member of this family is RhoA, which negatively controls neurite outgrowth (Govek et al., 2011) and whose prenylation allows its translocation to the plasma membrane and its subsequent activation (Segatto et al., 2014b). We tested whether Sim affected RhoA content in membrane fraction. As shown in Figure 18 Sim decreased RhoA levels in membrane lysates, and this effect was reverted by MVA and GG, indicating that Sim-induced neurite growth was mediated, at least in part, *via* reduced RhoA isoprenylation.

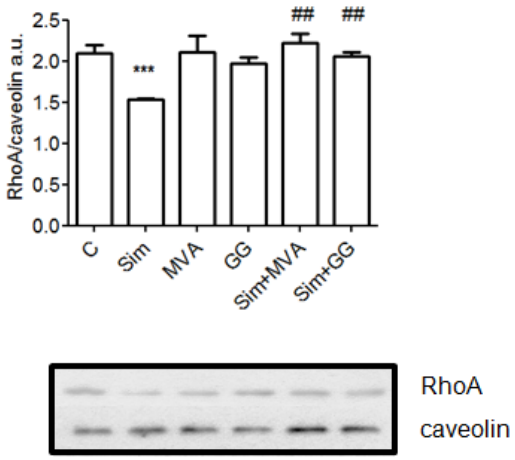

Figure 18. RhoA analysis in undifferentiated and differentiated N1E-115 mouse neuroblastoma in presence of Sim and HMGCR end-products. N1E-115 cells were treated with 1 µM Sim, or 1 µM MVA, or 1 µM GG, or Sim + MVA, or Sim + GG for 120 h after DMSO administration. Then cell membranes were prepared as illustrated in the main text. Bottom of the figure shows an immunoblot from a representative experiment. Similar results were obtained from three independent experiments. Average protein expression is represented on the top and quantified as ratio between RhoA and caveolin. ***=P<0.001 vs. C, ##=P<0.01 vs. Sim as from one-way analysis of variance (ANOVA) followed by Tukey post-test.

Collectively, our data suggest that during neuronal differentiation, the activity of the MVA pathway decreases and we postulate that any interference with this process impacts neuronal morphology and function.

4.2 Altered brain cholesterol/isoprenoid metabolism in a rat model of autism spectrum disorders

(Cartocci et al., 2018 NEUROSCIENCE)

Once ascertained that MVA pathway is involved in neuron development we were aimed at knowing whether a neurodevelopmental disease such as autism could present altered MVA and cholesterol metabolism. Thus, our second aim was to study the possible modulation of MVA pathway and cholesterol metabolism, in a well-established animal model of autism induced by xenobiotics: rats prenatally exposed to valproic acid (VPA). To elucidate connections between ASDs and cholesterol/isoprenoid metabolism, we studied the protein network controlling cholesterol/isoprenoid homeostasis in different brain areas of infant, adolescent and adult male rats prenatally exposed to VPA.

We first ensured that VPA-exposed animals displayed autistic-like symptoms compared to control rats (Figure 19). At infancy (PND 9), pups prenatally exposed to VPA emitted less USVs than control pups when separated from the dam and the siblings (Figure 19a) indicating communicative deficits induced by prenatal VPA exposure. The elevated plus maze test revealed increased anxiety in VPA-exposed adolescent rats (PND 35) as indicated by decreased time spent in the open arms of the maze (Figure 19b) and a decreased number of open arm entries (Figure 19c) compared to SAL-exposed rats. The three-chamber test revealed decreased sociability in adolescent (Figure 19d) and adult (PND 90) (Figure 19e) rats as indicated by decreased time spent sniffing the stimulus animal during test compared to SAL-exposed animals (Figure 19e). However, the two groups did not differ in locomotor activity as shown by similar closed arm entries (data not shown).

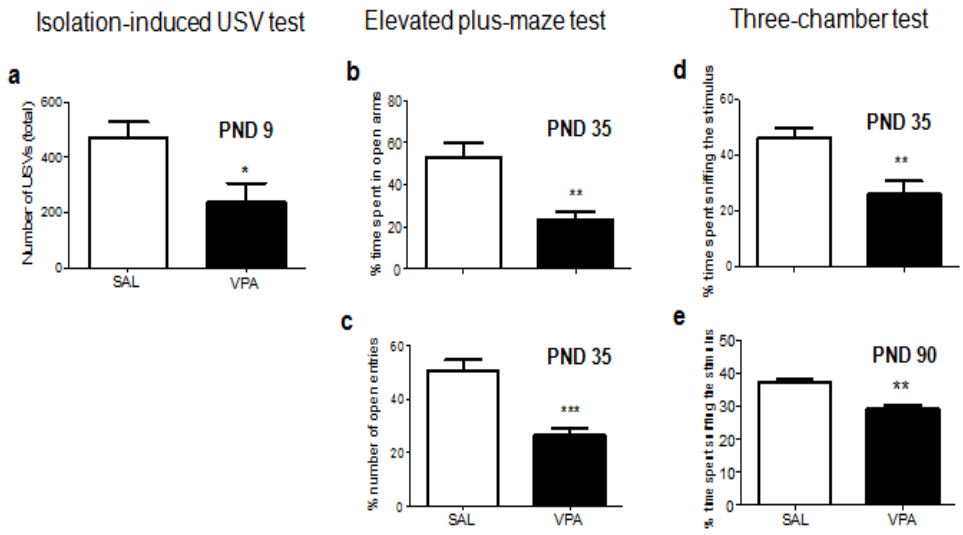

Figure 19. Behavioral tests in infant, adolescent, and adult rats prenatally exposed to VPA. Behavioral results obtained in infant rats (PND 9) tested in the isolation-induced USV test (**a**), in adolescent rats (PND 35) tested in the elevated plus-maze test (**b-c**) and in adolescent and adult (PND 90) rats tested in the three-chamber test (**d-e**)

We then studied the impact of VPA on liver and plasma cholesterol homeostasis (Figure 20). Our analysis revealed that VPA exposure *per se* did not affect both total cholesterol and HDL levels in plasma (Figure 20a-b). Measurements in the liver, which is the metabolic power plant of lipid homeostasis (Trapani et al., 2012), showed a mild perturbation of proteins ensuring cholesterol homeostasis (Figure 20c-d-e-f) and of cholesterol content (Figure 20g) only in the VPA-exposed infant rats (PND 13), but no changes at older ages. Thus, prenatal VPA exposure altered hepatic cholesterol metabolism only transiently and left plasma levels unaffected.

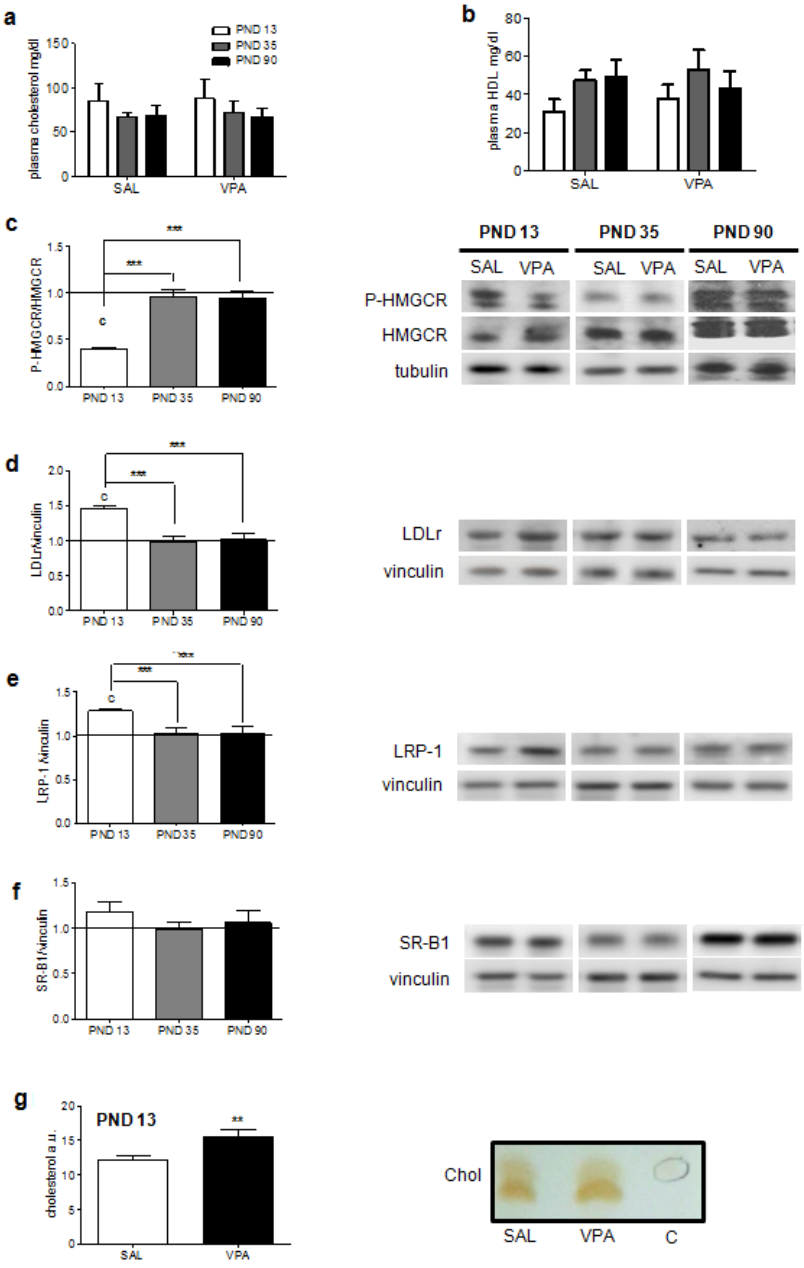

Figure 20. Peripheral cholesterol metabolism in infant, adolescent, and adult rats prenatally exposed to VPA. Levels of both plasma cholesterol and plasma HDL in infant, adolescent and adult rats respectively (**a**-**b**). The following four panels show the densitometric analysis (left) and a typical Western blots (right) of HMGCR phosphorylation state (**c**), and the protein levels of LDLr (**d**), LRP-1 (**e**), and SR-B1 (**f**). The densitometric analysis of Western blot is expressed as fold to SAL treated controls (1 value). Panel **g** illustrates the densitometric analysis and a typical TLC of cholesterol contents in livers of infant (PND 13) rats. The data are expressed as means ± SD of the arbitrary units obtained analyzing bands (from Western blots or TLC, for details see the main text) using the software ImageJ. The densitometric analysis are the mean of the results obtained from 6 different animals performed in duplicate. b $P<0.01$ vs SAL, c $P<0.001$ vs SAL as from a Student's t test. ***$P<0.001$ as from ANOVA followed by Tukey-Kramer test (GraphPad Instat3; GraphPad, Inc., La Jolla, CA).

We successively studied the protein network ensuring cholesterol/isoprenoid homeostasis in brain areas (amygdala, cerebellum, cortex, hippocampus, nucleus accumbens, and striatum) known to be involved in autism (Dichter et al., 2010; Donovan and Basson, 2017; Reim et

al., 2017; Wu et al., 2017) (Figure 21). To start, HMGCR and LDLr protein levels were measured in each brain region, since they are key components of cellular cholesterol homeostasis. Prenatal VPA exposure reduced HMGCR levels in the cortex and the nucleus accumbens of infant and adolescent rats, respectively, whereas all other brain areas were unaffected (Figure 21a). LDLr (Figure 21b) was significantly reduced in nucleus accumbens at all ages tested, decreased in the striatum of infant rats and enhanced in the cortex of adult animals. The fact that HMGCR content appeared largely unaffected by VPA does not exclude changes in enzyme activity, which is controlled at the posttranslational level by phosphorylation. Therefore, we investigated the phosphorylation status of HMGCR. Our data revealed that prenatal VPA induced region- and age-dependent changes in the ratio of P-HMGCR to total enzyme levels (Figure 21c). The cortex, for example, showed an age-dependent reversal of the VPA effect: whereas in young mice P-HMGCR/HMGCR ratio was reduced thereby increasing activity, adult mice showed the opposite effect. Interestingly, prenatal VPA exposure had the strongest impact on adolescent rats, where the ratio was altered in 5 out of 6 brain areas.

To further explore these changes, we measured the activation state (phosphorylation) of AMPK. Our immunoblots revealed that VPA-related changes in AMPK phosphorylation strongly corroborated the phosphorylation state of HMGCR (Figure 21d). These results suggested that VPA affected HMGCR activity *via* a signaling cascade involving AMPK rather than at transcriptional level. This is further supported by the fact that changes in HMGCR and LDLr were not correlated, although the transcription of both components is controlled by the common transcription factor SREBP-2.

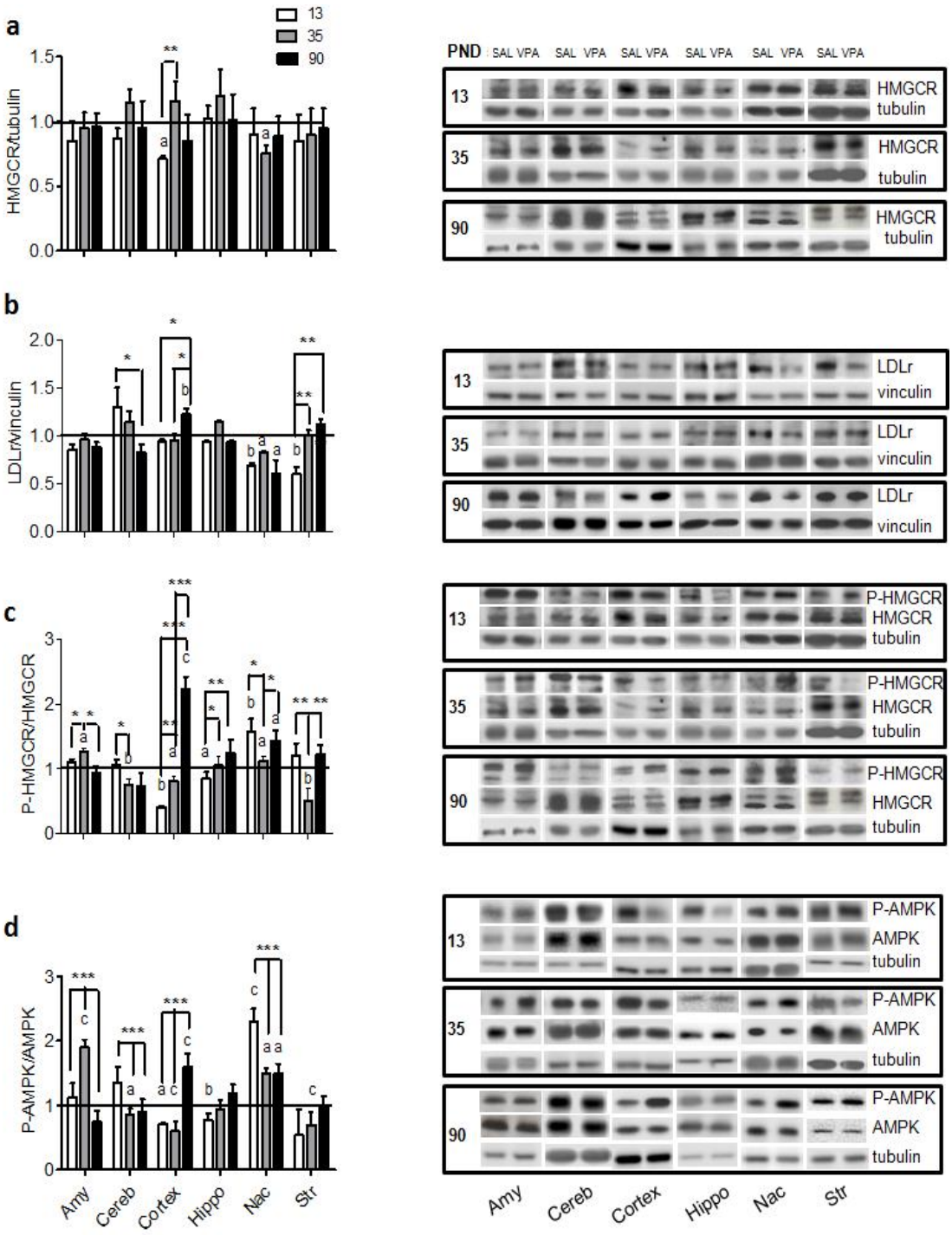

Figure 21. Proteins involved in cholesterol/isoprenoid homeostasis in the brain of infant, adolescent, and adult rats prenatally exposed to VPA or SAL. Densitometric analysis (left) and typical Western blot (right) of total HMGCR (**a**), LDLr (**b**), HMGCR phosphorylation state (**c)** and AMPK phosphorylation state (**d**) in indicated brain regions of infant (PND 13), adolescent (PND 35) and adult (PND 90) rats prenatally exposed to VPA or SAL. Western blot analysis shows proteins levels in SAL and VPA rats. The densitometric analysis of Western blot is expressed as fold of change of VPA treated versus SAL treated (1 value) rats. The data are expressed as means ± SD of the arbitrary units obtained analyzing bands (from Western blots, for details see the main text) using the software ImageJ. The densitometric analysis are the mean of the results obtained from 6 different animals performed in duplicate. a=P<0.05 vs SAL; b=P<0.01 vs SAL; c=P<0.001 vs SAL as from a Student's t test; *P<0.05 **P<0.01 ***P<0.001 as from ANOVA followed by Tukey-Kramer test (GraphPad Instat3; GraphPad, Inc., La Jolla, CA).

We also measured the levels of LRP-1 and SR-B1. Our data show that VPA affected LRP-1 levels in each brain area tested, but with distinct age-dependent patterns. Whereas levels in amygdala were enhanced in infant rats and decreased in adult mice, the levels in the cortex showed exactly the opposite changes (Figure 22a). SR-B1 was altered in all areas in an age-dependent manner except for cortex and the nucleus accumbens (Figure 22b). Together, these results indicated highly region- and age-specific effects of VPA on the different components of cholesterol/isoprenoid homeostasis. The good correlation between phosphorylation states of HMGCR and AMPK levels suggests that VPA induces AMPK-mediated changes in HMGCR activity in all regions of adolescent rats except for hippocampus. Among the lipoprotein receptors, LRP-1 levels were strongly affected by VPA in a region- and age-dependent manner.

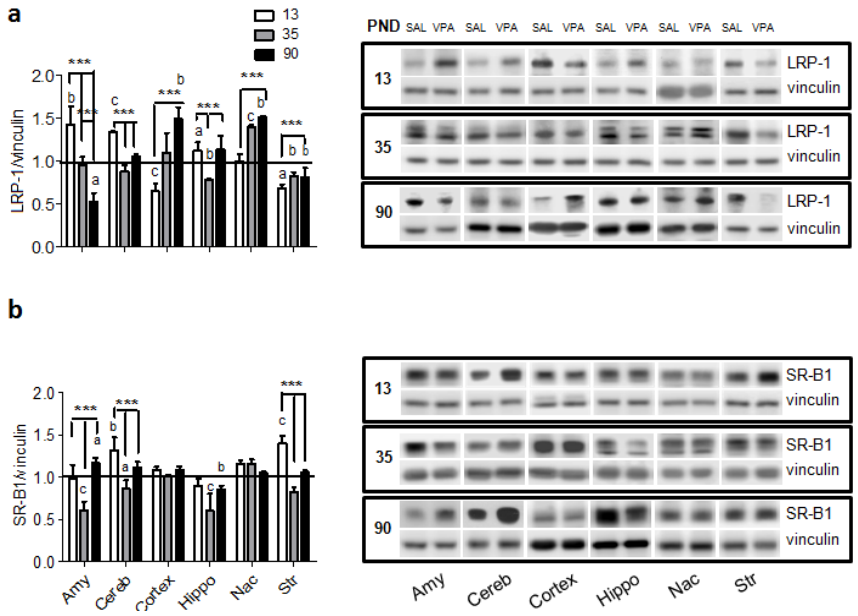

Figure 22. Receptors involved in cholesterol/isoprenoid homeostasis in the brain of infant, adolescent and adult rats prenatally exposed to VPA or SAL. LRP-1 (**a**) and SR-B1 (**b**) expression in indicated brain regions of infant (PND 13), adolescent (PND 35) and adult (PND 90) rats prenatally exposed to VPA or SAL. Western blot analysis shows proteins levels in SAL and VPA rats. The densitometric analysis of Western blot is expressed as fold of change of VPA treated versus SAL treated (1 value) rats. The data are expressed as means ± SD of the arbitrary units obtained analyzing bands (from Western blots, for details see the main text) using the software ImageJ. The densitometric analysis are the mean of the results obtained from 6 different animals performed in duplicate. a=P<0.05 vs SAL; b=P<0.01 vs SAL; c=P<0.001 vs SAL as from a Student's t test; ***P<0.001 as from ANOVA followed by Tukey-Kramer test (GraphPad Instat3; GraphPad, Inc., La Jolla, CA).

To test whether the VPA-induced alterations in HMGCR activity impacted the levels of its products, we analyzed cholesterol content in brain regions of adolescent rats using quantitative thin-layer chromatography. As shown in Figure 23a, we found that prenatal VPA exposure induced a significant reduction of cholesterol in the hippocampus, but not in any other region tested. In parallel, we studied the impact of VPA on the levels of geranylgeranyl and farnesyl. As an indirect measure, we determined the levels of membrane-attached RhoA and Ras comparing them to the amount of the proteins in the total lysate. Post-translational attachment of geranylgeranyl and farnesyl residues to these proteins induces their transition to the plasma membrane. Prenatal VPA exposure strongly increased and decreased the levels of membrane-attached RhoA (Figure 23b) and Ras (Figure 23c) in the cerebellum and nucleus accumbens, respectively. Moreover, the content of membrane-bound Ras was reduced in the striatum. Interestingly, the total protein content did not change except for the nucleus accumbens in which an increase of the total RhoA and Ras was observed, probably due to a compensatory action of the tissue.

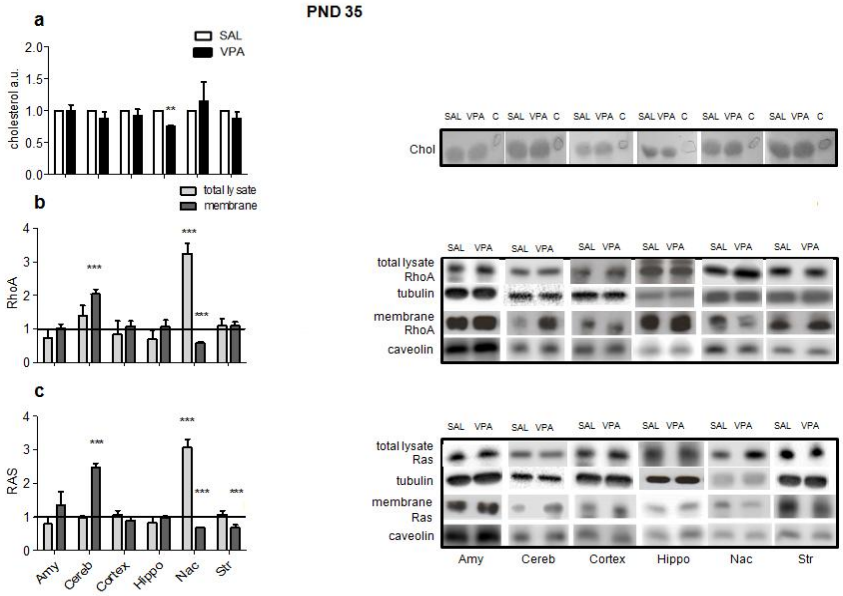

Figure 23. Cholesterol and expression levels of membrane-bound Ras and RhoA in different brain areas of VPA- or SAL-exposed adolescent (PND 35) rats. Densitometric analysis (left) and a typical TLC (right) of cholesterol content (**a**) in different brain areas of VPA- or SAL-exposed adolescent (PND 35) rats. The following panels show the densitometric analysis (left) and a typical Western blot (right) of RhoA total lysate and membrane content (**b**) and the Ras total lysate and membrane content (**c**) in indicated brain region of SAL and VPA exposed adolescent rats (PND 35). The densitometric analysis of Western blot is expressed as fold of change of VPA treated versus SAL treated (1 value) rats. For details see the main text. The data are expressed as means ± SD of the arbitrary units obtained analyzing the bands using the software ImageJ. The densitometric analysis are the mean of the results obtained from 6 different animals performed in duplicate. **P<0.01 and ***P<0.001 as from a Student's t test vs SAL (1 value).

Prenatal VPA exposure markedly reduced cholesterol levels in the hippocampus of adolescent rats. Since most cholesterol in the brain is contained in myelin, we assessed whether VPA reduced myelin content in the hippocampus using myelin basic protein (MBP) as marker. As shown in Figure 24a, VPA reduced MBP levels. The reduction of myelin content could have several causes. Based on published evidence that VPA inhibits differentiation of oligodendrocytes (Shen et al., 2008), we investigated the density of oligodendrocytes in the hippocampus. Immunohistochemical staining for Olig2, an oligodendrocyte-specific transcription factor, revealed a VPA-induced reduction of Olig2 immunopositive ($Olig2^{+}$) cells in the CA1 and CA2 areas (Figure 24b-c-d) indicating that myelin reduction is caused by VPA-induced inhibition of oligodendrocyte formation.

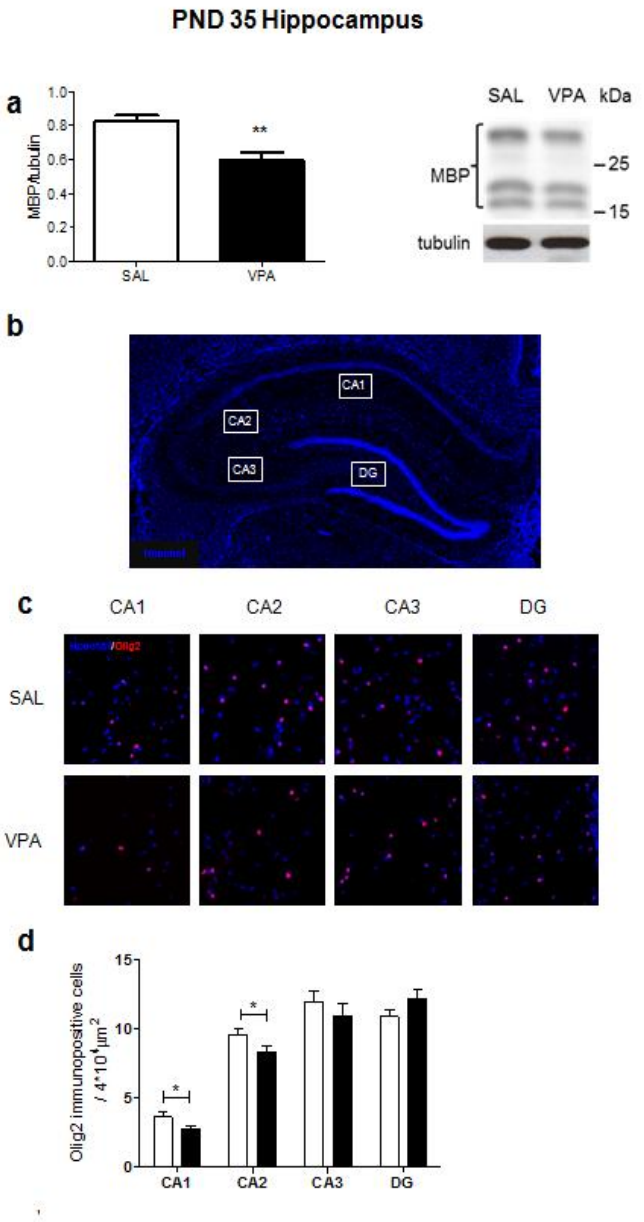

Figure 24. MBP protein content and oligodendrocytes immunofluorescence in hippocampi of VPA- or SAL-exposed adolescent (PND 35) rats. Densitometric analysis (left) and a typical Western blot (right) of MBP content (**a)** in the hippocampus of VPA- or SAL-exposed adolescent rats (PND 35). For details see the main text. (**b**) Exemplifying photomicrograph of the entire hippocampus which shows the sub-regions analyzed (magnification 4X). (**c**) Representative fluorescent photomicrographs of Olig2 (red) staining performed in the stratum radiatum of CA1, CA2, CA3, and in the hilus of the DG regions of hippocampi of SAL- and VPA-exposed PND 35 rats (magnification 20X). (**d**) Cell count analysis expressed as $Olig2^+$ cells/4×10^4 μm^2. Nuclei were stained with Hoechst (blue). The data are expressed as means ± SD for Western blot experiments, and means ± SEM for immunofluorescence experiments. Images were analyzed using the software ImageJ. The densitometric analyses are the mean of the results obtained from 6 different animals performed in duplicate. The cell count analysis is representative of three different experiments performed in quadruplicate. *P<0.05 vs SAL; **P<0.01 vs SAL as from a Student's t test.

In conclusion, our results reveal that prenatal exposure to VPA provokes long-lasting region- and age-specific changes in brain cholesterol/isoprenoid homeostasis and thereby support the hypothesis that autistic-like symptoms could be caused by alterations in cholesterol/isoprenoid metabolism in the brain.

4.3 Sex dependent differences of cholesterol metabolism modulation in rats prenatally exposed to valproate

(Cartocci et al., manuscript in preparation)

Since cholesterol metabolism is differently regulated in male and female (Trapani and Pallottini, 2010) and ASDs display a sex-dependent incidence, my third aim was to study putative sex-dependent alterations in brain cholesterol metabolism. Thus, we analyzed male and female adolescent and adult rats by using the same experimental animal model employed before. We avoided infants since hormonal sex-dependent changes are not present at 9-13 days.

We started to study the consequence of the VPA treatment on plasma cholesterol levels in PND 35 and PND 90 animals. Our results showed, as already demonstrated (De Marinis et al., 2008) that female rats have a lower level of cholesterolemia and that VPA does not affect plasma cholesterol levels either in male or in female animals both at PND 35 and PND 90 (Figure 25).

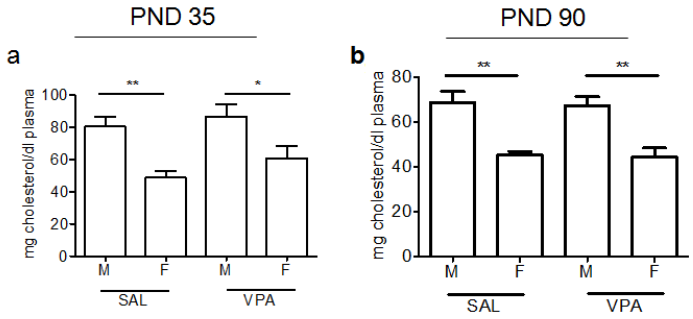

Figure 25. Plasma cholesterol levels in adolescent and adult male and female rats prenatally exposed to VPA. Levels of plasma cholesterol in adolescent and adult rats respectively (**a-b**). The data are expressed as means ± SD. The results have been obtained from 6 different animals for both sexes performed in duplicate. *P<0.05, **P<0.001 as from ANOVA followed by Tukey-Kramer test (GraphPad Instat3; GraphPad, Inc., La Jolla, CA).

Moreover, we evaluated VPA effects on the main proteins controlling cholesterol metabolism in the liver at both ages. HMGCR and LDLr levels were quantified through Western blot analysis: Figure 26 illustrates that VPA *per se* did not alter both proteins levels despite, as already observed, females show higher HMGCR phosphorylation levels than males (Figure 26a-b) accompanied by a rise in LDLr expression (Figure 26b-c).

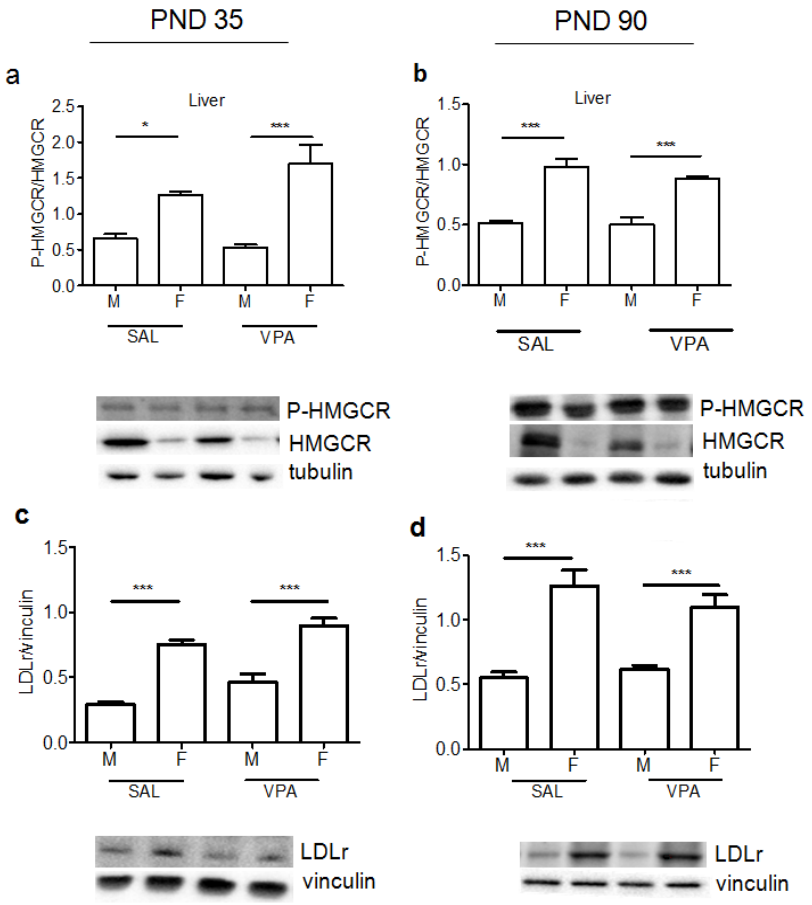

Figure 26. Peripheral cholesterol metabolism in adolescent and adult male and female rats prenatally exposed to VPA. The figures illustrate the densitometric analysis of HMGCR phosphorylation state in PND 35 (**a**) and PND 90 (**b**), and the protein levels of LDLr in PND 35 (**c**) and PND 90 (**d**). The data are expressed as means ± SD of the arbitrary units obtained analyzing bands (from Western blots) using the software ImageJ. The results are obtained from 6 different animals, the experiments were performed in duplicate. ***P<0.001 vs SAL as from ANOVA followed by Tukey-Kramer test (GraphPad Instat3; GraphPad, Inc., La Jolla, CA).

Then, after establishing that VPA did not modify plasma and liver cholesterol homeostasis, our attention was focused on the protein network controlling cholesterol homeostasis in the same brain areas analyzed before. We analyzed HMGCR, LDLr, LRP-1 and SR-B1. It is interesting to note that these proteins, in most of the studied areas display different levels in male and female in SAL exposed animals, as observable the Western blots of each figure. This underlies a sex-, age-, and tissue-specific cholesterol metabolism regulation. Regarding the responses of the different brain areas to VPA treatment, we can observe that total HMGCR does not change either in male and in female at PND 90 (Figure 27b), while in PND 35 animals some changes are observable: for instance, VPA showed a decrease of

HMGCR levels in cortex and hippocampus from female rats and in nucleus accumbens of male rats (Figure 27a).

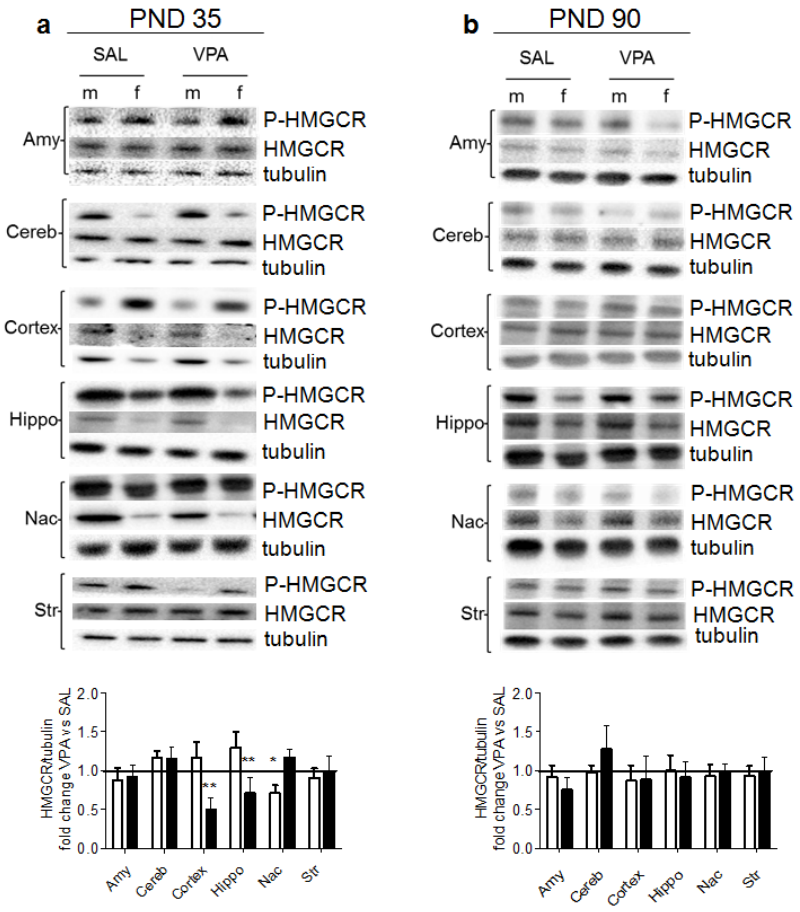

Figure 27. HMGCR levels in the brain of adolescent, and adult male and female rats prenatally exposed to VPA or SAL. Densitometric analysis of total HMGCR (**a**,**b**) in male (white bars) and female (black bars)in indicated brain regions of adolescent (PND 35) and adult (PND 90) rats prenatally exposed to VPA or SAL. The densitometric analysis of Western blot is expressed as fold of change of VPA treated versus SAL treated (1 value) rats. The data are expressed as means ± SD of the arbitrary units obtained analyzing bands (from Western blots) using the software ImageJ. The densitometric analysis are the mean of the results obtained from 6 different animals performed in duplicate. *P<0.05 **P<0.01 as from Student's t test (GraphPad Instat3; GraphPad, Inc., La Jolla, CA).

At PND 35, LDLr (Figure 28a) shows the same alterations observed for HMGCR except in the hippocampus, on the contrary at PND 90 this protein is altered mainly in male where four out of six areas are affected. Females show an alteration only in the cerebellum (Figure 28b).

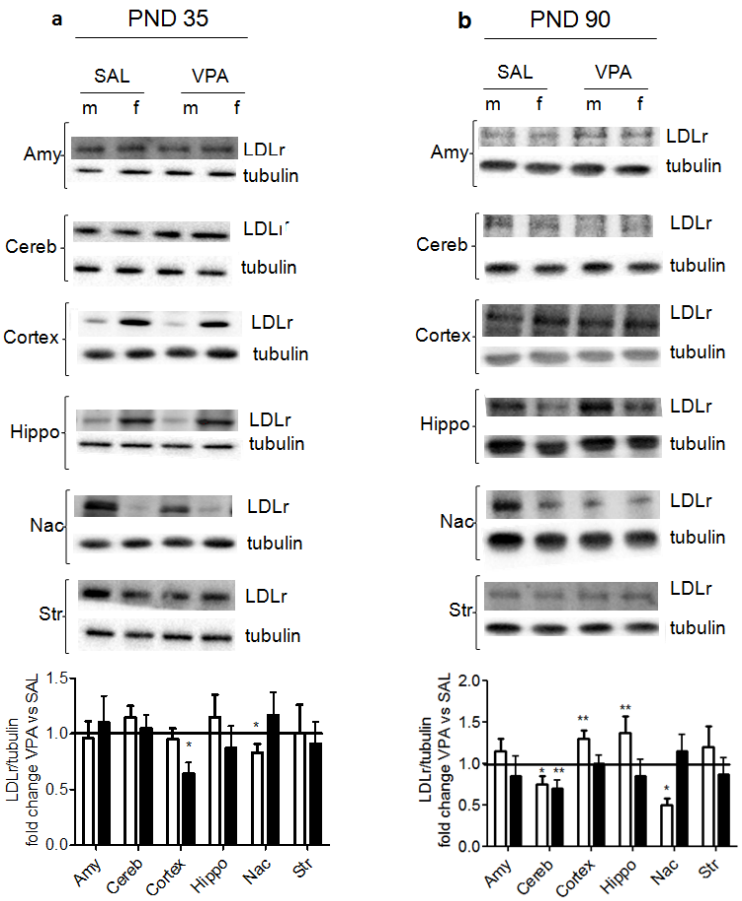

Figure 28. LDLr levels in the brain of adolescent, and adult male and female rats prenatally exposed to VPA or SAL. Densitometric analysis of LDLr (**a-b**) in male (white bars) and female (black bars) in indicated brain regions of adolescent (PND 35) and adult (PND 90) rats prenatally exposed to VPA or SAL. The densitometric analysis of Western blot is expressed as fold of change of VPA treated versus SAL treated (1 value) rats. The data are expressed as means ± SD of the arbitrary units obtained analyzing bands (from Western blots) using the software ImageJ. The densitometric analysis are the mean of the results obtained from 6 different animals performed in duplicate. *P<0.05 **P<0.01 as from Student's t test (GraphPad Instat3; GraphPad, Inc., La Jolla, CA).

VPA-dependent age- and sex-variations were particularly prominent for HMGCR phosphorylation. In particular, PND 35 results to be the most affected age, showing alterations in all the studied areas with dimorphic effects. At this age, HMGCR phosphorylation is increased in amygdala and decreased in cerebellum upon VPA exposure, and only cerebellum maintains this trend also in PND 90. Interestingly, no sex-dependent differences were detectable in these brain areas at both developmental states. On the contrary, cortex, hippocampus, nucleus accumbens, and striatum respond to VPA in different manner in both adolescence and adulthood (Figure 29a-b).

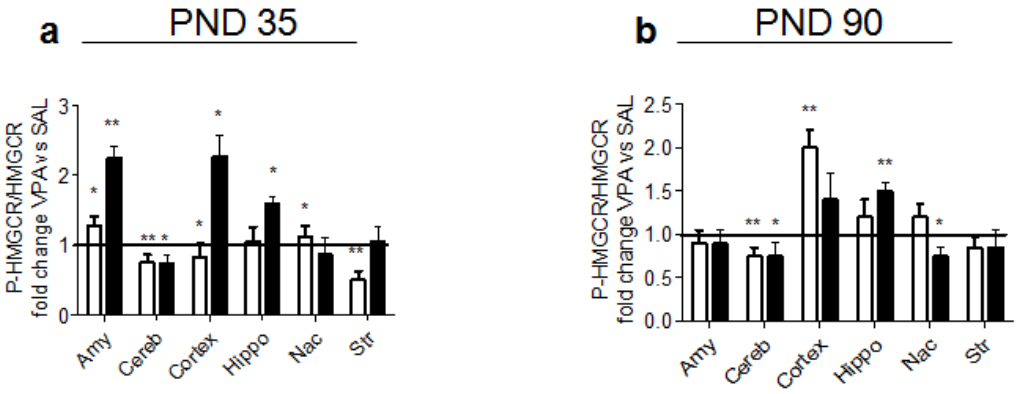

Figure 29. HMGCR phosphorylation state in the brain of adolescent, and adult male and female rats prenatally exposed to VPA or SAL. Densitometric analysis of HMGCR phosphorylation state in male (white bars) and female (black bars) in indicated brain regions of adolescent (PND 35) and adult (PND 90) rats prenatally exposed to VPA or SAL in PND 35 (**a**) and PND 90 (**b**). The data are expressed as means ± SD of the arbitrary units obtained analyzing bands (from Western blots) using the software ImageJ. The densitometric analysis are the mean of the results obtained from 6 different animals performed in duplicate. *P<0.05 **P<0.01 as from Student's t test (GraphPad Instat3; GraphPad, Inc., La Jolla, CA).

Considering that cholesterol cellular content is regulated by synthesis and uptake mechanisms, we analyzed also the levels of other two receptors involved in these important processes, LRP-1 and SR-B1 proteins.

Immunoblot analysis showed that LRP-1 level was decreased in VPA male only during the adulthood in amygdala and cerebellum, while in VPA female rats the protein expression changed in both adolescence and adult age, but affecting different brain areas (Figure 30a-b).

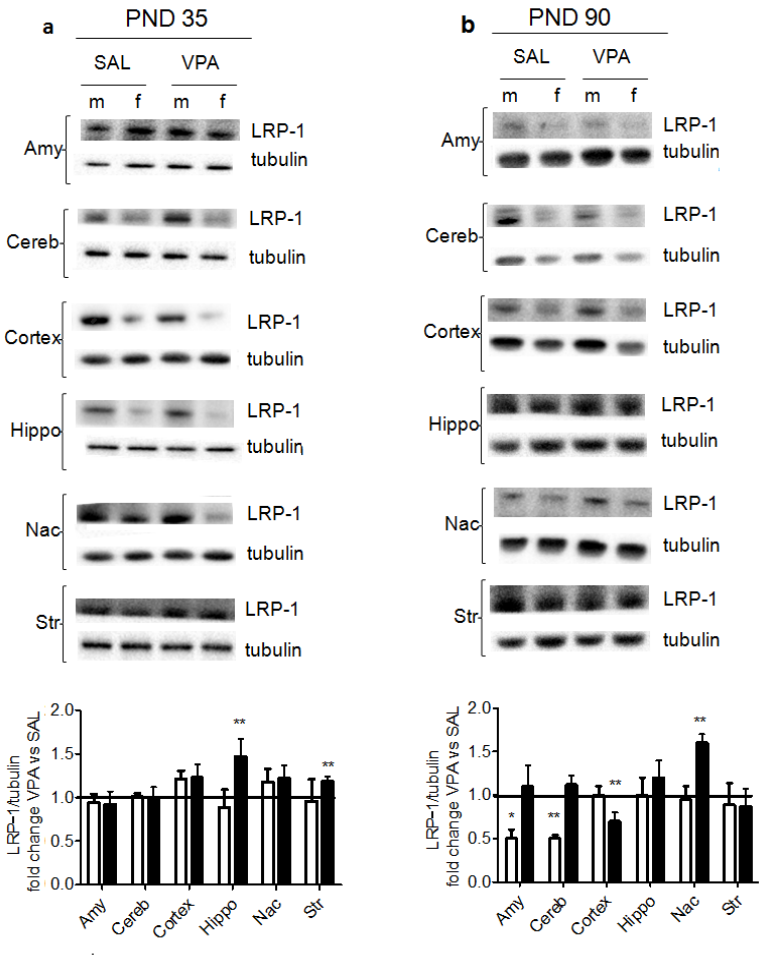

Figure 30. LRP-1 receptor levels in the brain of adolescent and adult male and female rats prenatally exposed to VPA or SAL. LRP-1 (**a-b**) in indicated brain regions of infant male (white bars) and female (black bars) adolescent (PND 35) and adult (PND 90) rats prenatally exposed to VPA or SAL. The densitometric analysis of Western blot is expressed as fold of change of VPA treated versus SAL treated (1 value) rats. The data are expressed as means ± SD of the arbitrary units obtained analyzing bands (from Western blots) using the software ImageJ. The densitometric analysis are the mean of the results obtained from 6 different animals performed in duplicate. *P<0.05 **P<0.01 as from Student's t test (GraphPad Instat3; GraphPad, Inc., La Jolla, CA).

SR-B1 levels were also modulated in a sex-dependent manner: PND 35 VPA males showed a more evident response to the treatment, since they manifest alterations in three brain areas, (cerebellum, hippocampus and amygdala). The amygdala is the only altered region in adolescent female rats. Interestingly, at PND 90 the treatment affected more females than males, in fact VPA exposed females displayed decreased SR-B1 levels in four of six brain areas, (amygdala, cortex, hippocampus and striatum), while males underwent changes only in cerebellum and cortex (Figure 31a-b).

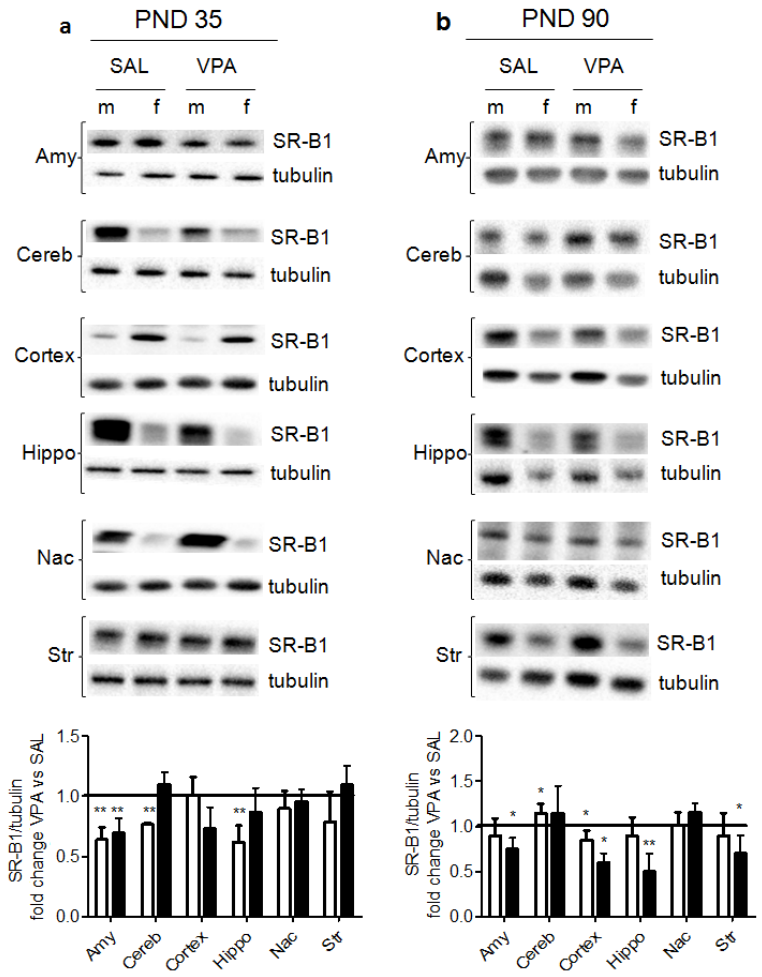

Figure 31. SR-B1 receptor levels in the brain of adolescent and adult male and female rats prenatally exposed to VPA or SAL. SR-B1(**a-b**) in indicated brain regions of infant male (white bars) and female (black bars) adolescent (PND 35) and adult (PND 90) rats prenatally exposed to VPA or SAL. The densitometric analysis of Western blot is expressed as fold of change of VPA treated versus SAL treated (1 value) rats. The data are expressed as means ± SD of the arbitrary units obtained analyzing bands (from Western blots,) using the software ImageJ. The densitometric analysis are the mean of the results obtained from 6 different animals performed in duplicate. *P<0.05 **P<0.01 as from Student's t test (GraphPad Instat3; GraphPad, Inc., La Jolla, CA).

Overall, our results confirm that sex-dependent modulations of cholesterol metabolism in liver and plasma are present in rats. Our Western blots measurements show that these differences are also observable in the brain of SAL-treated rats. Moreover, the results highlight that the different brain areas respond in a sex-dependent manner to prenatal exposure to VPA.

CHAPTER 5

DISCUSSION

Autism spectrum disorders (ASD) are a group of neurodevelopmental disabilities characterized by difficulties in social interaction, communication, restricted and repetitive interests and behaviors, and in many cases by a delay of cognitive functions. Since the symptoms of autism occur during the early childhood, in particular during brain development, it has been hypothesized that these disorders, are related with an imbalance between excitatory and inhibitory synapses, alterations during neurite outgrowth or the elongation of axons and dendrites (Auerbach et al., 2011; Zoghbi and Bear, 2012; Delorme et al., 2013; Wang and Doering, 2013; Bakos et al., 2015). Interestingly, patients affected by ASDs, such as Smith Lemli Optiz Syndrome or Asperger Syndrome show, among the different features, alterations of plasma cholesterol homeostasis. The occurrence of imbalanced cholesterol synthesis and/or transport has been hypothesized in the brain of ASD patients (Wang, 2014; Tierney, 2006). Despite these observations, no systematic studies on the protein network of cholesterol homeostasis maintenance in neurodevelopmental disorders have been performed. Thus, the main goals of this thesis were i) to study the role of MVA pathway and the modulation of the protein network of cholesterol homeostasis during neuronal differentiation, ii) to study, in ASD experimental models, the protein network of cholesterol homeostasis in different brain areas; iii) to identify whether sex-related differences are present in the same experimental model of autism since ASDs are characterized by a ratio 4:1 between male and female (Werling and Geschwind, 2013).

Neuronal differentiation is a decisive phase during brain development, characterized by different steps. The brain functions depend critically by the correct execution of these developmental events. Interference with neuronal differentiation due to genetic factors, drug treatment or environmental factors exposure can provoke late neurologic or psychiatric symptoms (Hill et al., 2015; Nuttall, 2015; Chaudhury et al., 2015). For this reasons, it is important to identify the metabolic pathways that are decisive for this process, and that are potentially involved in disease mechanisms. For this reason, we focused our attention on the protein network that controls the MVA pathway and in turn the cellular cholesterol homeostasis during neuronal differentiation. Intriguingly, HMGCR activation decreased along the considered time points, suggesting a progressive reduction of MVA pathway

activation during neuronal differentiation. This result is in good agreement with the hypothesis that during development, neurons decrease their cholesterol synthesis (Mauch et al., 2001; Pfrieger and Ungerer, 2011). The decrease of HMGCR activity is due to decline of the total protein levels and independent from phosphorylation/dephosphorylation mechanisms. The decrease of both transcription factors (SREBP-1 and -2) not only accounts for the reduced HMGCR protein expression, but also for the significant fall in LDLr (Horton, 2002) and for the increased LRP-1 levels (Llorente-Cortes et al., 2006; Llorente-Cortes et al., 2007). Regarding SR-B1 we did interesting observations. During differentiation the protein dimerizes leading to the appearance of a 150 kDa band. The dimerization represents a physiological event, since the protein is functional when expressed on the cell surface as a dimer (Gaidukov et al., 2011). Indeed, flow cytometric analysis, performed in live cells, does not show any SR-B1 signal on membrane surfaces of undifferentiated cells (0 h) whereas an increase of fluorescence intensity is detectable at 72 h in accordance with the appearance of the 150 kDa SR-B1 in Western blot analysis. Thus, since cholesterol synthesis decreases during neuronal differentiation, cells could supply their cholesterol needs through the increase of both LRP-1 and the functional SR-B1. In our opinion SR-B1 dimerization may be considered a new marker of neuronal differentiation. Our results show that the pharmacological inhibition of MVA pathway increases the rate of neurite outgrowth. These results are in good agreement with those obtained by other research groups (Maltese and Sheridan, 1985; Sato-Suzuki and Murota, 1996; Pooler et al., 2006; Holmberg et al., 2006; Raina et al., 2013). These effects are completely prevented by MVA administration, indicating that Sim-induced neurite elongation depends on the specific HMGCR inhibition and not by an effect exerted by Sim *per se*. Beside cholesterol, MVA is the precursor of isoprenoids such as GG or Far that are required for the prenylation and the subsequent activation of different proteins. The finding that only GG prevented the Sim-induced neurite outgrowth, suggests that geranylgeranylated proteins, rather than farnesylated ones or cholesterol, promote neurite formation and elongation. The intracellular cholesterol content did not change in differentiating cells both in presence and in absence of Sim. Moreover, we found that Sim significantly reduced membrane-associated RhoA levels in N1E-115 cells. Geranylgeranylation of RhoA is essential for membrane translocation and the activation of its signaling cascade (Seasholtz et al., 1999). This includes the actomyosin-based contractility of neurites and the disassembly of microtubules and intermediate filaments leading to neurite retraction (Hirose et al., 1998). We therefore conclude that

HMGCR inhibition promotes neurite elongation by preventing the activation of the negative regulator RhoA.

These data indicate that the decrease of the MVA pathway is fundamental for neurite outgrowth and in turn neuronal differentiation.

Since ASDs, that are neurodevelopmental disorders, have been related to isoprenoid/cholesterol homeostasis alterations, we decided to study the protein network controlling cholesterol/isoprenoid homeostasis in different brain areas of infant, adolescent and adult male rats prenatally exposed to VPA, a well-established rodent model for the disease (Tierney et al., 2006; Ruhela et al., 2015). Our results reveal that prenatal exposure to VPA provokes long-lasting region- and age-specific changes in brain cholesterol/isoprenoid homeostasis and thereby support the hypothesis that autistic-like symptoms could be caused by alterations in cholesterol/isoprenoid metabolism in the brain (Wang, 2014; Cartocci et al., 2017).

Our findings clearly underline that cholesterol homeostasis in the brain is vulnerable to pharmacologic manipulations. Whereas hepatic cholesterol metabolism was only transiently perturbed by prenatal VPA exposure, the brain showed a wide array of changes that occurred immediately or with delays of several weeks, that differed among brain regions and that occasionally reverted within a given brain area. This complex reaction indicates, as previously suggested (Segatto et al., 2011; Segatto et al., 2013), that cholesterol/isoprenoid metabolism is differently regulated in brain areas and supports recent findings that prenatal VPA exposure provokes region-and gene-specific reactions (Lauber et al., 2016). These regional differences may be due to region-specific cellular composition, namely the neuron/glia ratio, metabolic turnover and activity pattern. The levels of HMGCR and LDLr remained remarkably stable except for small changes that were surprisingly incongruent. Under normal conditions, both components are controlled by the SREBP-2 pathway, which tightly regulates cholesterol levels in cells. In case of a deficit, HMGCR and LDLr are upregulated to increase synthesis and uptake. The divergent changes induced by VPA argue against a robust activation of the SREBP-2 pathway and suggest that different post-transcriptional regulation can be present, such as diverse mRNA stability as already demonstrated (Pallottini et al., 2006).

Our study reveals that VPA affects the activation state of HMGCR as implied by changing levels of the phosphorylated form. In particular, during adolescence, prenatal VPA altered HMGCR activity in five out of six brain areas. This includes an increase in cerebellum, cortex, and striatum and a decrease in amygdala and nucleus accumbens. No changes were

observed in the hippocampus. The strong correlation between HMGCR activation state and the AMPK phosphorylation indicate that VPA acts *via* the AMPK-dependent pathway on cholesterol/isoprenoid metabolism. This is in line with previous evidence that VPA activates AMPK (Avery and Bumpus, 2014; Ji et al., 2015). However, in our experimental model AMPK was differently modulated in each brain area. Possible reasons are the involvement of other factors or regional differences in cell composition. Coherently with this observation previous findings demonstrated that each brain area responds differently to the same stimulus: as an example, rat hippocampus and cortex differently react to estradiol stimulation regarding HMGCR and LDLr expression (Segatto et al., 2011).

Our study revealed a strong impact of VPA on the membrane-associated fractions of Ras and RhoA and again, the direction of VPA-induced changes differed among brain regions. Their levels increased in the cerebellum, but decreased in the nucleus accumbens. In the case of the cerebellum, that is implicated in social cognition (Laidi et al., 2017), it is likely that the change occurred in granule cells, as these cells represent the main cell type in this brain area. A very recent paper suggests that cerebellar alteration may be related to eye avoidance and reduced social attention that are likely to be involved in the pathophysiology of ASDs (Laidi et al., 2017). Anyway, the functional impact of these changes remains almost unclear since small G proteins mediate a large number of cellular processes: an increase in prenylated Ras can impair long-term potentiation and has been associated with cognitive impairment (Hottman and Li, 2014; Mainberger et al., 2016). The increase in prenylated RhoA could alter proper neurite outgrowth and synaptic plasticity (Cartocci et al., 2016). Both proteins can be anchored at the membrane after posttranslational attachment of prenyl moieties, whose availability is controlled by HMGCR activity. Moreover, prenylated proteins have important roles in neuronal development and plasticity (Homberg et al., 2016). The analysis of adolescent rats revealed that prenatal VPA exposure decreased the cholesterol and myelin content in the hippocampus, whereas HMGCR was not activated. This reduction was probably due to a reduced number of oligodendrocytes. This observation is supported by published evidence that VPA inhibits the differentiation of oligodendrocytes (Dehghan et al., 2016; Pazhoohan et al., 2014; Ye et al., 2009). VPA is an inhibitor of Histone Deacetylases (HDACs), and it has been demonstrated that inhibition of HDACs decreases myelination and Schwann cell differentiation in the peripheral nervous system (Jacob et al., 2011; Brugger et al., 2017), it might induce epigenetic reprogramming, influencing cell types such as oligodendrocytes that are not even born at the time of injection (Bianchi et al., 2012). Our results reveal selective effects in the CA1 and CA2 regions of the

hippocampus explaining the decrease of cholesterol in the same areas (Caporali et al., 2016; Berghoff et al., 2017). At present, we cannot exclude, however, that the cholesterol content of neurons was reduced as well. This could impair their development and function, in particular at synaptic level as well as could impact on neuronal survival (Mauch et al., 2001; Shrivastava et al., 2010; Saxena and Chattopadhyay, 2012; Jafurulla et al., 2014). In this regard, in a recent paper, Wu and colleagues demonstrated that FTY720, an immunosuppressor used for treatment of multiple sclerosis, rescues VPA-induced autistic behavior exerting a direct protection of neuron survival (Wu et al., 2017). Very interestingly, this drug is also able to reduce cholesterol content in human fibroblasts as recently demonstrated by Newton and colleague (Newton et al., 2017), suggesting that cholesterol modulation could be really involved in ASDs, but further studies on specific cellular types in specific brain areas should necessarily be performed.

Interestingly, since the autistic features are more common in males than females with a ratio of 4:1 (Werling and Geschwind, 2013) and a preclinical study described a VPA gender-dependent response (Schneider et al., 2008), I finally decided to investigate in adolescent and adult male and female rats, prenatally exposed to VPA, the protein network regulating MVA pathway in the liver and brain. My results confirmed the sex-dependent differences of MVA pathway in the tissues under investigation (De Marinis et al., 2008; Segatto, 2011). VPA-exposure does not affect plasma cholesterol and MVA pathway in the liver. On the contrary, we found that VPA-exposure profoundly but differently affected the proteins regulating MVA pathway in the brain. As an example, while in adults VPA did not determine any alteration of total HMGCR levels either in male and female, in the adolescent animals, the treatment induced sex-dependent alterations in cortex, hippocampus, and nucleus accumbens. Significant LDLr alterations are mainly observable in adult male, where VPA differently affects four of six considered brain areas. Moreover, sex-dependent, tissue- and age-specific responses to prenatal VPA-exposure are present in the other proteins under investigations. These results underlie that the protein related to MVA pathway are regulated in a sex-dependent manner in each brain area by the same stimulus, confirming as already reported (Segatto et al., 2011).

CHAPTER 6

CONCLUDING REMARKS

Prenatal life is a critical and plastic period of development during which external insults lead to permanent changes in cells, tissues and even in the whole organs (Barker et al., 2002). In particular, maternal stressors during gestation are associated with gender-specific disturbances in neurodevelopment and brain morphology in the offspring leading to cognitive, behavioral and emotional problems in adult age (DiPietro, 2012). The data collected in this PhD thesis fit perfectly with these statements, in fact they demonstrate that the progressive decrease in the activation of MVA pathway is a physiological feature in differentiating neurons, and assume that any interference in the modulation of this metabolic pathway can alter neuronal functions and development. Coherently, this pathway and its regulatory network are altered in a preclinical model of neurodevelopmental diseases (ASDs) induced by a prenatal VPA exposure. Moreover, ASDs are more frequent in males than in females and, interestingly, the results show sex-dependent alterations of MVA pathway in the same experimental model.

Overall my work suggests that neurodevelopmental disorders induced by maternal-derived stressors are paralleled with sex-dependent MVA pathway alterations.

REFERENCES

Andersen OM, Vorum H, Honore B, Thogersen HC (2003) Ca2+ binding to complement-type repeat domains 5 and 6 from the low-density lipoprotein receptor-related protein. BMC biochemistry 4:7.

Auerbach BD, Osterweil EK, Bear MF (2011) Mutations causing syndromic autism define an axis of synaptic pathophysiology. Nature 480:63-68.

Avery LB, Bumpus NN (2014) Valproic acid is a novel activator of AMP-activated protein kinase and decreases liver mass, hepatic fat accumulation, and serum glucose in obese mice. Mol Pharmacol 85:1-10.

Bakos J, Bacova Z, Grant SG, Castejon AM, Ostatnikova D (2015) Are Molecules involved in Neuritogenesis and Axon Guidance Related to Autism Pathogenesis? Neuromolecular Med 17:297-304.

Barker DJ, Forsen T, Eriksson JG, Osmond C (2002) Growth and living conditions in childhood and hypertension in adult life: a longitudinal study. Journal of Hypertens 20:1951-1956.

Bentinger M, Tekle M, Dallner G (2010) Coenzyme Q--biosynthesis and functions. Biochem Biophys Res Commun 396:74-9.

Berghoff SA, Gerndt N, Winchenbach J, Stumpf SK, Hosang L, Odoardi F, Ruhwedel T, Bohler C, Barrette B, Stassart R, Liebetanz D, Dibaj P, Mobius W, Edgar JM, Saher G (2017) Dietary cholesterol promotes repair of demyelinated lesions in the adult brain. Nat Commun 8:14241.

Bianchi MG, Franchi-Gazzola R, Reia L, Allegri M, Uggeri J, Chiu M, Sala R, Bussolati O (2012) Valproic acid induces the glutamate transporter excitatory amino acid transporter-3 in human oligodendroglioma cells. Neuroscience 227:260-270.

Bos JL, Rehmann H, Wittinghofer A (2007) GEFs and GAPs: critical elements in the control of small G proteins. Cell 129:865-77.

Brandt U (1999) Proton translocation in the respiratory chain involving ubiquinone--a hypothetical semiquinone switch mechanism for complex I. BioFactors 9:95-101.

Brugger V, Duman M, Bochud M, Munger E, Heller M, Ruff S, Jacob C (2017) Delaying histone deacetylase response to injury accelerates conversion into repair Schwann cells and nerve regeneration. Nat Commun 8:14272.

Buchovecky CM, Turley SD, Brown HM, Kyle SM, McDonald JG, Liu B, Pieper AA, Huang W, Katz DM, Russell DW, Shendure J, Justice MJ (2013) A suppressor screen in Mecp2 mutant mice implicates cholesterol metabolism in Rett syndrome. Nature genetics 45:1013-1020.

Buhaescu I, Izzedine H (2007) Mevalonate pathway: a review of clinical and therapeutical implications. Clinical biochemistry 40:575-584.

Burg JS, Espenshade PJ (2011) Regulation of HMG-CoA reductase in mammals and yeast. Prog Lipid Res 50:403-10.

Cantagrel V, Lefeber DJ (2011) From glycosylation disorders to dolichol biosynthesis defects: a new class of metabolic diseases. Journal of inherited metabolic disease 34:859-867.

Caporali P, Bruno F, Palladino G, Dragotto J, Petrosini L, Mangia F, Erickson RP, Canterini S, Fiorenza MT (2016) Developmental delay in motor skill acquisition in Niemann-Pick C1 mice reveals abnormal cerebellar morphogenesis. Acta Neuropathol Commun 4:94.

Cartocci V, Segatto M, Di Tunno I, Leone S, Pfrieger FW, Pallottini V (2016) Modulation of the Isoprenoid/Cholesterol Biosynthetic Pathway During Neuronal Differentiation In Vitro. J Cell Biochem 117:2036-2044.

Cartocci V, Servadio M, Trezza V, Pallottini V (2017) Can Cholesterol Metabolism Modulation Affect Brain Function and Behavior? J Cell Physiol.

Casey PJ, Seabra MC (1996) Protein prenyltransferases. J Biol Chem 271:5289-92.

Chaudhury S, Sharma V, Kumar V, Nag TC, Wadhwa S (2015) Activity-dependent synaptic plasticity modulates the critical phase of brain development. Brain Dev 38:355-63.

Chojnacki T, Dallner G (1988) The biological role of dolichol. The Biochemical journal 251:1-9.

Christensen DL, Baio J, Van Naarden Braun K, Bilder D, Charles J, Constantino JN, Daniels J, Durkin MS, Fitzgerald RT, Kurzius-Spencer M, Lee LC, Pettygrove S, Robinson C, Schulz E, Wells C, Wingate MS, Zahorodny W, Yeargin-Allsopp M, Centers for Disease C, Prevention (2016) Prevalence and Characteristics of Autism Spectrum Disorder Among Children Aged 8 Years--Autism and Developmental Disabilities Monitoring Network, 11 Sites, United States, 2012. Morbidity and mortality weekly report Surveillance summaries 65:1-23.

Clejan S, Dotson RS, Wolf EW, Corb MP, Ide CF (1996) Morphological differentiation of N1E-115 neuroblastoma cells by dimethyl sulfoxide activation of lipid second messengers. Exp Cell Res 224:16-27.

Coleman and Gillberg (2011)The autisms Oxford University Press, USA, 05 gen 2012

De Marinis E, Martini C, Trentalance A, Pallottini V (2008) Sex differences in hepatic regulation of cholesterol homeostasis. J Endocrinol 198:635-43.

DeBose-Boyd RA (2008) Feedback regulation of cholesterol synthesis: sterol-accelerated ubiquitination and degradation of HMG CoA reductase. Cell Res 18:609-21.

Defesche JC (2004) Low-density lipoprotein receptor--its structure, function, and mutations. Semin Vasc Med 4:5-11.

Dehghan S, Hesaraki M, Soleimani M, Mirnajafi-Zadeh J, Fathollahi Y, Javan M (2016) Oct4 transcription factor in conjunction with valproic acid accelerates myelin repair in demyelinated optic chiasm in mice. Neuroscience 318:178-189.

Delorme R, Ey E, Toro R, Leboyer M, Gillberg C, Bourgeron T (2013) Progress toward treatments for synaptic defects in autism. Nature medicine 19:685-694.

Dhar MK, Koul A, Kaul S (2013) Farnesyl pyrophosphate synthase: a key enzyme in isoprenoid biosynthetic pathway and potential molecular target for drug development. New biotechnology 30:114-123.

Dichter GS, Felder JN, Green SR, Rittenberg AM, Sasson NJ, Bodfish JW (2010) Reward circuitry function in autism spectrum disorders. Soc Cogn Affect Neurosci 7:160-172.

Dipietro JA (2012) Maternal stress in pregnancy: considerations for fetal development. J Adolesc Health 51:S3-8.

Doimo M, Desbats MA, Cerqua C, Cassina M, Trevissom E, Salviati L (2014) Genetics of coenzyme q10 deficiency. Molecular syndromology 5:156-162.

Donovan AP, Basson MA (2017) The neuroanatomy of autism - a developmental perspective. J Anat 230:4-15.

Dziobek I, Gold SM, Wolf OT, Convit A (2007) Hypercholesterolemia in Asperger syndrome: independence from lifestyle, obsessive-compulsive behavior, and social anxiety. Psychiatry research 149:321-324.

Elias ER, Irons MB, Hurley AD, Tint GS, Salen G (1997) Clinical effects of cholesterol supplementation in six patients with the Smith-Lemli-Opitz syndrome (SLOS). American journal of medical genetics 68:305-310.

Emonard H, Théret L, Bennasroune AH, Dedieu S (2014) Regulation of LRP-1 expression: make the point. Pathol Biol (Paris) 62:84-90.

Enrich C, Rentero C, Hierro A, Grewal T (2015) Role of cholesterol in SNARE-mediated trafficking on intracellular membranes. Journal of cell science 128:1071-1081.

Faras H, Al Ateeqi N, Tidmarsh L (2010) Autism spectrum disorders. Annals of Saudi medicine 30:295-300.

Festenstein GN, Heaton FW, Lowe JS, Morton RA (1955) A constituent of the unsaponifiable portion of animal tissue lipids (lambda max. 272 m mu). The Biochemical journal 59:558-566.

Friesen JA, Rodwell VW (2004) The 3-hydroxy-3-methylglutaryl coenzyme-A (HMG-CoA) reductases. Genome Biol 5:248.

Gaidukov L, Nager AR, Xu S, Penman M, Krieger M (2011) Glycine dimerization motif in the N-terminal transmembrane domain of the high density lipoprotein receptor SR-BI required for normal receptor oligomerization and lipid transport. J Biol Chem 286:18452-18464.

Gent J, Braakman I (2004) Low-density lipoprotein receptor structure and folding. Cell Mol Life Sci 61:2461-70.

Gillberg C, Fernell E, Kocovska E, Minnis H, Bourgeron T, Thompson L, Allely CS (2017) The role of cholesterol metabolism and various steroid abnormalities in autism spectrum disorders: A hypothesis paper. Autism research : official journal of the International Society for Autism Research 10:1022-1044.

Gillott A, Standen PJ (2007) Levels of anxiety and sources of stress in adults with autism. J Intellect Disabil 11:359-370.

Govek EE, Hatten ME, Van Aelst L (2011) The role of Rho GTPase proteins in CNS neuronal migration. Dev Neurobiol 71:528-553.

Hannoush RN, Sun J (2010) The chemical toolbox for monitoring protein fatty acylation and prenylation. Nat Chem Biol 6:498-506.

Harisa GI, Alanazi FK (2014) Low density lipoprotein bionanoparticles: From cholesterol transport to delivery of anti-cancer drugs. Saudi Pharm J 22:504-15.

Herz J (2001) The LDL receptor gene family: (un)expected signal transducers in the brain. Neuron 29:571-581.

Herz J, Strickland DK (2001) LRP: a multifunctional scavenger and signaling receptor. The Journal of clinical investigation 108:779-784.

Hill DS, Cabrera R, Wallis Schultz D, Zhu H, Lu W, Finnell RH, Wlodarczyk BJ (2015) Autism-Like Behavior and Epigenetic Changes Associated with Autism as Consequences of In Utero Exposure to Environmental Pollutants in a Mouse Model. Behav Neurol 2015:426263.

Hirose M, Ishizaki T, Watanabe N, Uehata M, Kranenburg O, Moolenaar WH, Matsumura F, Maekawa M, Bito H, Narumiya S (1998) Molecular dissection of the Rho-associated protein kinase (p160ROCK)-regulated neurite remodeling in neuroblastoma N1E-115 cells. J Cell Biol 141:1625-1636.

Holmberg E, Nordstrom T, Gross M, Kluge B, Zhang SX, Doolen S (2006) Simvastatin promotes neurite outgrowth in the presence of inhibitory molecules found in central nervous system injury. J Neurotrauma 23:1366-1378.

Homberg JR, Kyzar EJ, Nguyen M, Norton WH, Pittman J, Poudel MK, Gaikwad S, Nakamura S, Koshiba M, Yamanouchi H, Scattoni ML, Ullman JF, Diamond DM, Kaluyeva AA, Parker MO, Klimenko VM, Apryatin SA, Brown RE, Song C, Gainetdinov RR, Gottesman, II, Kalueff AV (2016) Understanding autism and other neurodevelopmental disorders through experimental translational neurobehavioral models. Neurosci Biobehav Rev 65:292-312.

Horton JD (2002) Sterol regulatory element-binding proteins: transcriptional activators of lipid synthesis. Biochem Soc Trans 30:1091-1095.

Hottman DA, Li L (2014) Protein prenylation and synaptic plasticity: implications for Alzheimer's disease. Mol Neurobiol 50:177-185.

Istvan ES, Palnitkar M, Buchanan SK, Deisenhofer J (2000) Crystal structure of the catalytic portion of human HMG-CoA reductase: insights into regulation of activity and catalysis. EMBO J 19:819-30.

Istvan ES, Deisenhofer J (2000) The structure of the catalytic portion of human HMG-CoA reductase. Biochim Biophys Acta 1529:9-18.

Jacob C, Christen CN, Pereira JA, Somandin C, Baggiolini A, Lotscher P, Ozcelik M, Tricaud N, Meijer D, Yamaguchi T, Matthias P, Suter U (2011) HDAC1 and HDAC2 control the transcriptional program of myelination and the survival of Schwann cells. Nat Neurosci 14:429-436.

Jafurulla M, Rao BD, Sreedevi S, Ruysschaert JM, Covey DF, Chattopadhyay A (2014) Stereospecific requirement of cholesterol in the function of the serotonin1A receptor. Biochim Biophys Acta 1838:158-163.

Ji MM, Wang L, Zhan Q, Xue W, Zhao Y, Zhao X, Xu PP, Shen Y, Liu H, Janin A, Cheng S, Zhao WL (2015) Induction of autophagy by valproic acid enhanced lymphoma cell chemosensitivity through HDAC-independent and IP3-mediated PRKAA activation. Autophagy 11:2160-2171.

Kanekiyo T, Bu G (2014) The low-density lipoprotein receptor-related protein 1 and amyloid-beta clearance in Alzheimer's disease. Front Aging Neurosci 6:93.

Kinoshita M, Fujita M, Usui S, Maeda Y, Kudo M, Hirota D, Suda T, Taki M, Okazaki M, Teramoto T (2004) Scavenger receptor type BI potentiates reverse cholesterol transport system by removing cholesterol ester from HDL. Atherosclerosis 173:197-202.

Krieger M (2001) Scavenger receptor class B type I is a multiligand HDL receptor that influences diverse physiologic systems. Journal of Clinical Investigation 108:793-797.

Lai MC, Lombardo MV, Baron-Cohen S (2014) Autism. Lancet 383:896-910.

Laidi C, Boisgontier J, Chakravarty MM, Hotier S, d'Albis MA, Mangin JO, Devenyi GA, Delorme R, Bolognani F, Czech C, Bouquet C, Toledano E, Bouvard M, Gras D, Petit J, Mishchenko M, Gaman A, Scheid I, Leboyer M, Zalla T, Houenou J (2017) Cerebellar anatomical alterations and attention to eyes in autism. Sci Rep 7:12008.

Lauber E, Filice F, Schwaller B (2016) Prenatal Valproate Exposure Differentially Affects Parvalbumin-Expressing Neurons and Related Circuits in the Cortex and Striatum of Mice. Front Mol Neurosci 9:150.

Lecis C, Segatto M (2014) Cholesterol Homeostasis Imbalance and Brain Functioning: Neurological Disorders and Behavioral Consequences. Journal of Neurology and Neurological Disorders 1:101.

Lillis AP, Mikhailenko I, Strickland DK (2005) Beyond endocytosis: LRP function in cell migration, proliferation and vascular permeability. J Thromb Haemost 3:1884-93.

Lillis AP, Van Duyn LB, Murphy-Ullrich JE, Strickland DK (2008) LDL receptor-related protein 1: unique tissue-specific functions revealed by selective gene knockout studies. Physiol Rev 88:887-918.

Llorente-Cortes V, Costales P, Bernues J, Camino-Lopez S, Badimon L (2006) Sterol regulatory element-binding protein-2 negatively regulates low density lipoprotein receptor-related protein transcription. J Mol Biol 359:950-960.

Llorente-Cortes V, Royo T, Otero-Vinas M, Berrozpe M, Badimon L (2007) Sterol regulatory element binding proteins downregulate LDL receptor-related protein (LRP1) expression and LRP1-mediated aggregated LDL uptake by human macrophages. Cardiovasc Res 74:526-536.

Lord C, Risi S, DiLavore PS, Shulman C, Thurm A, Pickles A (2006) Autism from 2 to 9 years of age. Archives of general psychiatry 63:694-701.

Lowry OH, Rosebrough NJ, Farr AL, Randall RJ (1951) Protein measurement with the Folin phenol reagent. J Biol Chem 193:265-275.

Luo DX, Cao DL, Xiong Y, Peng XH, Liao DF (2010) A novel model of cholesterol efflux from lipid-loaded cells. Acta Pharmacol Sin 31:1243-57.

Lutjohann D, von Bergmann K (2003) 24S-hydroxycholesterol: a marker of brain cholesterol metabolism. Pharmacopsychiatry 36 Suppl 2:S102-106.

Mainberger F, Langer S, Mall V, Jung NH (2016) Impaired synaptic plasticity in RASopathies: a mini-review. J Neural Transm (Vienna) 123:1133-1138.

Maltese WA, Sheridan KM (1985) Differentiation of neuroblastoma cells induced by an inhibitor of mevalonate synthesis: relation of neurite outgrowth and acetylcholinesterase activity to changes in cell proliferation and blocked isoprenoid synthesis. J Cell Physiol 125:540-558.

Manduca A, Morena M, Campolongo P, Servadio M, Palmery M, Trabace L, Hill MN, Vanderschuren LJ, Cuomo V, Trezza V (2015) Distinct roles of the endocannabinoids anandamide and 2-arachidonoylglycerol in social behavior and emotionality at different developmental ages in rats. Eur Neuropsychopharmacol 25:1362-1374.

Markram K, Rinaldi T, La Mendola D, Sandi C, Markram H (2008) Abnormal fear conditioning and amygdala processing in an animal model of autism. Neuropsychopharmacology 33:901-912.

Martini C, Pallottini V (2007) Cholesterol: from feeding to gene regulation. Genes Nutr 2:181-93.

Martín MG, Pfrieger F, Dotti CG (2014) Cholesterol in brain disease: sometimes determinant and frequently implicated. EMBO Rep 15:1036-52

Mauch DH, Nagler K, Schumacher S, Goritz C, Muller EC, Otto A, Pfrieger FW (2001) CNS synaptogenesis promoted by glia-derived cholesterol. Science 294:1354-1357.

Mintz M (2017) Evolution in the Understanding of Autism Spectrum Disorder: Historical Perspective. Indian journal of pediatrics 84:44-52.

Mitsche MA, McDonald JG, Hobbs HH, Cohen JC (2015) Flux analysis of cholesterol biosynthesis in vivo reveals multiple tissue and cell-type specific pathways. eLife 4:e07999.

Miziorko HM (2011) Enzymes of the mevalonate pathway of isoprenoid biosynthesis. Archives of biochemistry and biophysics 505:131-143.

Moy SS, Nadler JJ, Young NB, Perez A, Holloway LP, Barbaro RP, Barbaro JR, Wilson LM, Threadgill DW, Lauder JM, Magnuson TR, Crawley JN (2007) Mouse behavioral tasks relevant to autism: phenotypes of 10 inbred strains. Behav Brain Res 176:4-20.

Morell and Quarles (1999) Characteristic composition of myelin. Basic neurochemistry: molecular, cellular and medical aspects. 6th edition.

Newton J, Hait NC, Maceyka M, Colaco A, Maczis M, Wassif CA, Cougnoux A, Porter FD, Milstien S, Platt N, Platt FM, Spiegel S (2017) FTY720/fingolimod increases NPC1 and NPC2 expression and reduces cholesterol and sphingolipid accumulation in Niemann-Pick type C mutant fibroblasts. FASEB J 31:1719-1730.

Nicolini C, Fahnestock M (2017) The valproic acid-induced rodent model of autism. Experimental neurology.

Nowicka B, Kruk J (2010) Occurrence, biosynthesis and function of isoprenoid quinones. Biochimica et biophysica acta 1797:1587-1605.

Nuttall JR (2015) The plausibility of maternal toxicant exposure and nutritional status as contributing factors to the risk of autism spectrum disorders. Nutr Neurosci 20:209-218.

Oh JE, Karlmark Raja K, Shin JH, Pollak A, Hengstschlager M, Lubec G (2006) Cytoskeleton changes following differentiation of N1E-115 neuroblastoma cell line. Amino Acids 31:289-298.

Olson RE (1998) Discovery of the lipoproteins, their role in fat transport and their significance as risk factors. The Journal of nutrition 128:439S-443S.

Pallottini V, Guantario B, Martini C, Totta P, Filippi I, Carraro F, Trentalance A (2008) Regulation of HMG-CoA reductase expression by hypoxia. J Cell Biochem 104:701-709.

Pallottini V, Martini C, Cavallini G, Donati A, Bergamini E, Notarnicola M, Caruso MG, Trentalance A (2006) Modified HMG-CoA reductase and LDLr regulation is deeply involved in age-related hypercholesterolemia. J Cell Biochem 98:1044-1053.

Paxinos G, Watson C (2007) The rat brain in stereotaxic coordinates. Academic Press, USA 6th Edition.

Pazhoohan S, Satarian L, Asghari AA, Salimi M, Kiani S, Mani AR, Javan M (2014) Valproic Acid attenuates disease symptoms and increases endogenous myelin repair by recruiting neural stem cells and oligodendrocyte progenitors in experimental autoimmune encephalomyelitis. Neurodegener Dis 13:45-52.

Pfrieger FW (2003a) Outsourcing in the brain: do neurons depend on cholesterol delivery by astrocytes? BioEssays : news and reviews in molecular, cellular and developmental biology 25:72-78.

Pfrieger FW (2003b) Role of cholesterol in synapse formation and function. Biochimica et biophysica acta 1610:271-280.

Pfrieger FW, Ungerer N (2011) Cholesterol metabolism in neurons and astrocytes. Progress in lipid research 50:357-371.

Pooler AM, Xi SC, Wurtman RJ (2006) The 3-hydroxy-3-methylglutaryl co-enzyme A reductase inhibitor pravastatin enhances neurite outgrowth in hippocampal neurons. J Neurochem 97:716-723.

Raina V, Gupta S, Yadav S, Surolia A (2013) Simvastatin induced neurite outgrowth unveils role of cell surface cholesterol and acetyl CoA carboxylase in SH-SY5Y cells. PLoS One 8:e74547.

Rauthan M, Pilon M (2011) The mevalonate pathway in C. elegans. Lipids in health and disease 10:243.

Reim D, Distler U, Halbedl S, Verpelli C, Sala C, Bockmann J, Tenzer S, Boeckers TM, Schmeisser MJ (2017) Proteomic Analysis of Post-synaptic Density Fractions from Shank3 Mutant Mice Reveals Brain Region Specific Changes Relevant to Autism Spectrum Disorder. Front Mol Neurosci 10:26.

Rip JW, Rupar CA, Chaudhary N, Carroll KK (1981) Localization of a dolichyl phosphate phosphatase in plasma membranes of rat liver. The Journal of biological chemistry 256:1929-1934.

Rodrigues JM, Luis AL, Lobato JV, Pinto MV, Faustino A, Hussain NS, Lopes MA, Veloso AP, Freitas M, Geuna S, Santos JD, Mauricio AC (2005) Intracellular Ca2+ concentration in the N1E-115 neuronal cell line and its use for peripheric nerve regeneration. Acta Med Port 18:323-328.

Rozman D, Monostory K (2010) Perspectives of the non-statin hypolipidemic agents. Pharmacology & therapeutics 127:19-40.

Ruhela RK, Prakash A, Medhi B (2015) An urgent need for experimental animal model of autissm in drug development. Annals of neurosciences 22:44-49.

Saddar S, Mineo C, Shaul PW (2010) Signaling by the high-affinity HDL receptor scavenger receptor B type I. Arterioscler Thromb Vasc Biol 30:144-50.

Saher G, Brugger B, Lappe-Siefke C, Mobius W, Tozawa R, Wehr MC, Wieland F, Ishibashi S, Nave KA (2005) High cholesterol level is essential for myelin membrane growth. Nature neuroscience 8:468-475.

Sato-Suzuki I, Murota S (1996) Simvastatin inhibits the division and induces neurite-like outgrowth in PC12 cells. Neurosci Lett 220:21-24.

Saxena R, Chattopadhyay A (2012) Membrane cholesterol stabilizes the human serotonin(1A) receptor. Biochim Biophys Acta 1818:2936-2942.

Schneider T, Roman A, Basta-Kaim A, Kubera M, Budziszewska B, Schneider K, Przewłocki R (2008) Gender-specific behavioral and immunological alterations in an animal model of autism induced by prenatal exposure to valproic acid. Psychoneuroendocrinology 33:728-40.

Scuderi C, Stecca C, Valenza M, Ratano P, Bronzuoli MR, Bartoli S, Steardo L, Pompili E, Fumagalli L, Campolongo P (2014) Palmitoylethanolamide controls reactive gliosis and exerts neuroprotective functions in a rat model of Alzheimer's disease. Cell Death Dis 5:e1419.

Seasholtz TM, Majumdar M, Brown JH (1999) Rho as a mediator of G protein-coupled receptor signaling. Mol Pharmacol 55:949-956.

Segatto M, Di Giovanni A, Marino M, Pallottini V (2013) Analysis of the protein network of cholesterol homeostasis in different brain regions: an age and sex dependent perspective. Journal of cellular physiology 228:1561-1567.

Segatto M, Leboffe L, Trapani L, Pallottini V (2014a) Cholesterol homeostasis failure in the brain: implications for synaptic dysfunction and cognitive decline. Current medicinal chemistry 21:2788-2802.

Segatto M, Manduca A, Lecis C, Rosso P, Jozwiak A, Swiezewska E, Moreno S, Trezza V, Pallottini V (2014b) Simvastatin treatment highlights a new role for the isoprenoid/cholesterol biosynthetic pathway in the modulation of emotional reactivity and cognitive performance in rats. Neuropsychopharmacology : official publication of the American College of Neuropsychopharmacology 39:841-854.

Segatto M, Trapani L, Lecis C, Pallottini V (2012) Regulation of cholesterol biosynthetic pathway in different regions of the rat central nervous system. Acta physiologica 206:62-71.

Segatto M, Trapani L, Marino M, Pallottini V (2011) Age- and sex-related differences in extra-hepatic low-density lipoprotein receptor. J Cell Physiol 226:2610-2616.

Servadio M, Melancia F, Manduca A, di Masi A, Schiavi S, Cartocci V, Pallottini V, Campolongo P, Ascenzi P, Trezza V (2016) Targeting anandamide metabolism rescues core and associated autistic-like symptoms in rats prenatally exposed to valproic acid. Translational Psychiatry.

Sever N, Yang T, Brown MS, Goldstein JL, DeBose-Boyd RA (2003) Accelerated degradation of HMG CoA reductase mediated by binding of insig-1 to its sterol-sensing domain. Molecular cell 11:25-33.

Shen S, Sandoval J, Swiss VA, Li J, Dupree J, Franklin RJ, Casaccia-Bonnefil P (2008) Age-dependent epigenetic control of differentiation inhibitors is critical for remyelination efficiency. Nat Neurosci 11:1024-1034.

Shepherd J, Cobbe SM, Ford I, Isles CG, Lorimer AR, MacFarlane PW, McKillop JH, Packard CJ (1995) Prevention of coronary heart disease with pravastatin in men with hypercholesterolemia. West of Scotland Coronary Prevention Study Group. The New England journal of medicine 333:1301-1307.

Shrivastava S, Pucadyil TJ, Paila YD, Ganguly S, Chattopadhyay A (2010) Chronic cholesterol depletion using statin impairs the function and dynamics of human serotonin(1A) receptors. Biochemistry 49:5426-5435.

Snipes GJ, Orfali W (1998) Common themes in peripheral neuropathy disease genes. Cell biology international 22:815-835.

Sooksawate T, Simmonds MA (2001) Effects of membrane cholesterol on the sensitivity of the GABA(A) receptor to GABA in acutely dissociated rat hippocampal neurones. Neuropharmacology 40:178-184.

Takai Y, Sasaki T, Matozaki T (2001) Small GTP-binding proteins. Physiological reviews 81:153-208.

Tierney E, Bukelis I, Thompson RE, Ahmed K, Aneja A, Kratz L, Kelley RI (2006) Abnormalities of cholesterol metabolism in autism spectrum disorders. American journal of medical genetics Part B, Neuropsychiatric genetics : the official publication of the International Society of Psychiatric Genetics 141B:666-668.

Tierney Aa (2008) Autism: the role of cholesterol in treatment. Int RevPsychiatry. Int RevPsychiatry 20:165-170.

Trapani L, Pallottini V (2010) Age-Related Hypercholesterolemia and HMG-CoA Reductase Dysregulation: Sex Does Matter (A Gender Perspective). Current gerontology and geriatrics research 420139.

Trapani L, Segatto M, Pallottini V (2012) Regulation and deregulation of cholesterol homeostasis: The liver as a metabolic "power station". World J Hepatol 4:184-190.

Trezza V, Damsteegt R, Manduca A, Petrosino S, Van Kerkhof LW, Pasterkamp RJ, Zhou Y, Campolongo P, Cuomo V, Di Marzo V, Vanderschuren LJ (2012) Endocannabinoids in amygdala and nucleus accumbens mediate social play reward in adolescent rats. J Neurosci 32:14899-14908.

Turunen M, Olsson J, Dallner G (2004) Metabolism and function of coenzyme Q. Biochimica et Biophysica Acta (BBA) - Biomembranes 1660:171-199.

Valacchi G, Sticozzi C, Lim Y, Pecorelli A (2011) Scavenger receptor class B type I: a multifunctional receptor. Annals of the New York Academy of Sciences 1229:E1-7.

van Deijk AF, Camargo N, Timmerman J, Heistek T, Brouwers JF, Mogavero F, Mansvelder HD, Smit AB, Verheijen MH (2017) Astrocyte lipid metabolism is critical for synapse development and function in vivo. Glia 65:670-682.

Vijayakumar NT, Judy MV (2016) Autism spectrum disorders: Integration of the genome, transcriptome and the environment. Journal of the neurological sciences 364:167-176.

Wang H (2014) Lipid rafts: a signaling platform linking cholesterol metabolism to synaptic deficits in autism spectrum disorders. Frontiers in behavioral neuroscience 8:104.

Wang H, Doering LC (2013) Reversing autism by targeting downstream mTOR signaling. Frontiers in cellular neuroscience 7:28.

Wennerberg K, Rossman KL, Der CJ (2005) The Ras superfamily at a glance. Journal of cell science 118:843-846.

Werling DM, Geschwind DH (2013) Sex differences in autism spectrum disorders. Current opinion in neurology 26:146-153.

Wu H, Wang X, Gao J, Liang S, Hao Y, Sun C, Xia W, Cao Y, Wu L (2017) Fingolimod (FTY720) attenuates social deficits, learning and memory impairments, neuronal loss and neuroinflammation in the rat model of autism. Life Sci 173:43-54.

Ye F, Chen Y, Hoang T, Montgomery RL, Zhao XH, Bu H, Hu T, Taketo MM, van Es JH, Clevers H, Hsieh J, Bassel-Duby R, Olson EN, Lu QR (2009) HDAC1 and HDAC2 regulate oligodendrocyte differentiation by disrupting the beta-catenin-TCF interaction. Nat Neurosci 12:829-838.

Zhai J, Bo Y, Lu Y, Liu C, Zhang L (2017) Effects of Coenzyme Q10 on Markers of inflammation: A Systematic Review and Meta-Analysis. PloS one 12:e0170172.

Zhang FL, Casey PJ (1996) Protein prenylation: molecular mechanisms and functional consequences. Annual review of biochemistry 65:241-269.

Zoghbi HY, Bear MF (2012) Synaptic dysfunction in neurodevelopmental disorders associated with autism and intellectual disabilities. Cold Spring Harbor perspectives in biology 4.

REPORT OF THE ACTIVITIES CARRIED ON DURING THE PhD

ACTIVITIES A.A 2014-2017	CFU (60 are mendatory)
Seminaries	24.5
Congresses	26.5
Courses	20
Total	**71**

Courses

- "Sicurezza in laboratorio" with final exam
- English (B2 level) with final exam
- "L'uso della statistica nella ricerca biomedica"
- Bioinformatic
- "The cerebellum inside-out: cells, circuits and functions" with poster presentation"

Oral Communications

- "Modulation of mevalonate pathway during neuronal differentiation" in the Annual Meeting of Young Researchers in Physiology, Florance, May 7- 9, 2015.
- "L'altra faccia degli interferenti endocrine: l'effetto anti colesterolemico di un flavonoide presente negli alimenti" in the National Convention INBB, Rome, October 22, 2015.
- "Brain cholesterol/isoprenoid metabolism is related to behavioral changes: autistic rats as experimental model", 11th Annual Meeting of Young Researchers, Florance May 25-27, 2017.
- "Autismo e colesterolo: c'è una relazione?", Notte Europea dei Ricercatori, Rome September 29, 2017.

Poster Presentations

- "Role of the endocannabinoid system in the behavioral abnormalities observed in the rat valproic acid model of autism" in the European Behavioral Pharmacology Society, Biennal Meeting, Verona, September 12-15, 2015.
- "Brain cholesterol metabolism changes in the valproic acid rat model of autism" in the PhD in Neuroscience National meeting, Naples, April 14-16, 2016.
- "Role of the endocannabinoid system in the altered social behavior observed in the rat valproic acid model of autism" in the European College of Neuropsycopharmacology, 29th Congress, Vienna, September17-20, 2016.
- "Alteration of cholesterol/isoprenoid homeostasis in the cerebellum of an experimental model of autism" in the International school of Brain Cells and Circuits "Camillo Golgi", during the course titled "The cerebellum inside-out: cells, circuits and functions", Erice, 1-5 December 2016.
- "Sex-related alterations of cholesterol homeostasis in a rat model of autism" in 2thNordic Neuroscience, Stockholm, 7-9 June 2017.

Publications

1. **Cartocci V**, Segatto M, Di Tunno I, Leone S, Pfrieger FW, Pallottini V. "Modulation of the Isoprenoid/Cholesterol Biosynthetic Pathway During Neuronal Differentiation In Vitro". *J Cell Biochem*. 2016 Sep;117(9):2036-44.
2. Servadio M, Melancia F, Manduca A, di Masi A, Schiavi S, **Cartocci V**, Pallottini V, Campolongo P, Ascenzi P, Trezza V. "Targeting anandamide metabolism rescues core and associated autistic-like symptoms in rats prenatally exposed to valproic acid". *Transl Psychiatry*. 2016 Sep 27;6(9):e902.
3. **Cartocci V**, Servadio M, Trezza V, Pallottini V. "Can Cholesterol Metabolism Modulation Affect Brain Function and Behavior?" *J Cell Physiol.* 2017 Feb;232(2):281-286.
4. **Cartocci V**, Catallo M, Tempestilli M, Segatto M, Pfrieger FV, Bronzuoli MR, Scuderi C, Servadio M, Trezza V, Pallottini V. "Altered brain cholesterol/isoprenoid metabolism in a rat model of autism spectrum disorders". *NEUROSCIENCE. 2018.*

5. **Cartocci V**, Di Pippo T, Vuono F, Schiavi S, Trezza V, Pallottini V. "Sex-dependent differences of cholesterol metabolism modulation in rats prenatally exposed to xenobiotics: the example of valproate". *In preparation.*
6. Schiavi S, Servadio M, Melancia F, **Cartocci V,** Pallottini V, Trezza V. "Autistic-like behavioral abnormalities observed in female rat prenatally exposed to valproic acid". *In preparation*

PhD Student

Tutor